

CHAPTER 1

INTRODUCTION

1.1 Introduction

With the accentuation on clean force age, the sustainable power based appropriated age frameworks have gotten incredible consideration. Bookkeeping to the ongoing advancements in photovoltaic innovation, the sunlight based photovoltaic (PV) based inexhaustible force age has encountered a quick development among the business and private areas [1]. Nonetheless, expanded dispersal of sun based PV power age into the customary lattice, has prompted different force quality issues, particularly in circulation networks where a critical segment of sustainable power sources are associated [2]. The coming of various force electronic loads additionally weakened the force quality in the organization. Different arrangements are proposed in the writing tending to the force quality issues without influencing the heap profile [2]-[3]. There is a long custom of utilizing direct regulators for power quality improvement in matrix interfaced frameworks anyway they have their own restrictions [4]. In addition, these control plans [4] require stage bolted circles (PLLs), which expands the framework multifaceted nature in common sense usage and prompts mal-activity under misshaped matrix voltages. As of late, the force quality improvement in the circulation matrix utilizing nonlinear modular prescient regulator (MPC), is mulled over by the creators in [5], nonetheless, its exhibition under nonlinear burdens, isn't explored. To improve power factor and to limit line current sounds, modular reference versatile control (MRAC) is presented in [6]. In any case, it requires information on reference framework from the earlier. These control systems [3]-[6] centre around improving the force quality in dissemination organization, with dynamic/responsive force infusion to the framework. Their activity under brace side issues, voltage unbalances and voltage symphonious mutilations isn't investigated.

Then again, there are control techniques for lattice interfaced inverters for ride through activity during adjusted/lopsided voltage droop issues, without zeroing in on the force quality improvement in the circulation matrix [7]-[14]. The specialists have accomplished the ride-through activity by infusing responsive force into the matrix. During the unbalance in conveyance lattice voltages, the guideline of matrix current gets testing. The control calculations are pondered to defeat this issue, either by adjusting the lattice flows or by limiting the dynamic force variances. For example, the creators in [7] have built up a fixed edge PQ regulator to limit the wave content in dynamic force through an addition

boundary. A coordinated edge current controller is pondered in [8]-[9] for power control during uneven lattice voltages. The usefulness of unequal voltage pay utilizing DG inverters is accounted for in [10]-[13], which depend on symmetric segments. In these control procedures, the DG inverters are controlled either through certain arrangement dynamic forces or positive grouping responsive forces [11]-[12] or both positive succession dynamic and receptive forces [10]-[13] for repaying the uneven voltages. The investigations have additionally been made for ride-through activity during lopsided voltage hangs with controllable dynamic/receptive force motions [15]-[18]. These techniques [7]-[18] portray distinctive control approaches for ride-through activity in network interfaced conveyed age frameworks during lattice voltage adjusted/uneven droops. Notwithstanding, a) they neglect to accomplish the force quality improvement in dispersion network through lattice current symphonious remuneration, b) they don't address the consonant/twisted framework voltages caused at far spiral finishes in the conveyance organization, and c) they neglect to address the elements of sustainable power asset, (for example, photovoltaic or wind) and the control of DC interface voltage. The elements in PV clusters, DC-DC power molding stage and the DC-interface capacitor, sway the activity of by and large framework, particularly during the deficiency ride through examination and thusly, the undertaking gets testing. The control techniques that consider elements of photovoltaic force plants are accounted for in [19]-[23]. The regulator [19] utilizes various corresponding resounding (PR) regulators to accomplish singular stage current remuneration. The framework execution with PR regulators, is corrupted under variety of the framework recurrence as it gives boundless addition at the chose symphonious frequencies. The non-ideal execution of limitless additions could cause arrangement of flimsiness issues for functional matrix interfaced DG frameworks [24]. Besides this, these methodologies [19]-[23] don't contribute for power quality improvement during nonlinear burdens and consonant voltages in the framework. In addition, the zero-succession and negative-arrangement powers are delivered by lopsided flows with unequal voltages, which gravely influence diverse business loads and modern burdens associated at the higher finish of the circulation framework, for example, three-stage engine loads/high force loads. The ride through activity of lattice interfaced PV frameworks under low voltage droops, which guarantees the distinctive force quality functionalities of consonant current alleviation, power factor amendment, adjusting of matrix flows, solid activity during unusual/symphonious network voltages caused in conveyance framework, is only occasionally announced in writing. In this paper, the EKF

plot based twofold stage network interfaced sun powered PV framework is proposed, to achieve complex targets. Right off the bat, the ride-through activity of framework interfaced twofold stage sun oriented PV framework is assessed under adjusted/uneven lattice side issues. During the framework blames, the PV inverter encourages the speedy identification and responds in like manner to limit the unfavorable consequences for the inverter and network side hardware, to follow IEEE Std. 1547.4. The framework encourages dynamic and responsive force infusion during the voltage-list deficiencies, so the PV frameworks stay operational under such conditions without bringing about additional hazards because of loss of PV age. Additionally, the proposed framework can withstand the matrix side symphonious/mutilated voltages by providing smooth and adjusted sinusoidal network flows. As opposed to numerous calculations on ride through activity, the proposed control technique can represent the nonlinear PCC loads in the dissemination framework, and makes up for the consonant flows infused into the lattice, in any event, during the shortcomings and symphonious voltage twists. Thusly, it fulfils the IEEE standard-519. The sinusoidal and adjusted network flows under all unsettling influences are guaranteed by fusing another path for extraction of unit-layouts of matrix voltages. This invalidates the negative arrangement and zero grouping power infusions into the network during the matrix voltage unbalances, along these lines, the impact of succession powers on modern/business loads, is invalidated. Other than this, a nonlinear Kalman channel is examined here. EKF is a numerical strategy, which works through expectation and revision component, and it gauges the basic of the heap current. It offers significantly better consistent state and dynamic exhibitions, over the straight regulators [25]-[26], under framework irritations. It is a factual strategy and doesn't require any dq-changes, which are inclined to mistakes if the simultaneous casing recognizable proof is mistaken, nor does it requires stage bolted circles. Its recursive structure permits constant execution without putting away perceptions or past appraisals. The principle commitments of the current work can be distinguished as follows.

- The flaw ride through control methodology is introduced for two phase lattice interfaced sun based PV framework that can deal with consonant/contorted matrix voltages, caused at far outspread closures in the circulation organization, and still inventory adjusted and sinusoidal network flows with THD with the cutoff points portrayed by IEEE Std. 519, in spite of serious voltage-list deficiencies.
- Contrary to a few control techniques on ride-through activity, this control procedure represents nonlinear burdens in the framework, and makes up for

unequal/symphonious burdens during the voltage-hang shortcomings and consonant voltages.

- EKF control appraises the principal load flows, without the earlier information on plentifulness, stage and conduct of the aggravations present in the heap flows. The prevalent consistent state and dynamic exhibitions of EKF based methodology over direct regulators are set up.

The framework is painstakingly assessed through re-enactments and analyses. A model of two-stage network interfaced PV framework is created in the lab and proposed control conspire is acknowledged utilizing DSP-dSPACE-1202 micro lab-box regulator. Test results approve the consistent state and dynamic exhibitions of the framework under various test conditions.

1.2 Literature Survey

Literature [1] portrays the joining of variable environmentally friendly power sources (RES) into power organizations. The fundamental objective is to stand up to the substance and patterns of logical writing with the eyes and undertakings of specialists on future themes and issues to be understood, particularly as far as the displaying of electrical frameworks. The examination depends on a bibliometric investigation of the Scopus information base on the subject and on an online study shipped off the relating creators of the distinguished papers. The paper investigates the elements of distribution, bunches of joint effort, and principle points considered. It at that point recognizes potential exploration leads, among which uncertain difficulties with respect to specialized angles, markets and financing issues, and social viewpoints. The divergence of models and results is as yet a vital insidious as exploration isn't full grown enough to incorporate in one model all the extremely perplexing boundaries of VRE mix into power frameworks. There is an absence of repeat, however, for example, the effect of new advancements or the improvement of substitute low carbon-emanating innovation (other than sun powered and wind), should be tended to.

Literature [2] depicts Maintaining a steady degree of intensity quality in the dissemination network is a developing test because of expanded utilization of intensity hardware converters in home grown, business and mechanical areas. Force quality disintegration is showed in expanded misfortunes; helpless usage of circulation frameworks; mal-activity of touchy gear and aggravations to close by purchasers, defensive gadgets, and correspondence frameworks. In any case, as the energy-sparing advantages will bring

about expanded AC power handled through force hardware converters, there is a convincing requirement for improved comprehension of relief procedures for power quality issues.

Literature [3] presents a multipurpose three stage twofold stage matrix interfaced photovoltaic (GPV) framework utilizing a versatile nonlinear control methodology. Alongside a pinnacle power extraction from a photovoltaic (PV) cluster, the proposed framework is equipped for sounds flows end, responsive force remuneration, matrix flows adjusting and versatile DC interface voltage control. The principal and music data from the dirtied load current are definitely assessed utilizing a versatile onlooker. A carefully certain genuine (SPR) Lyapunov's work is utilized to infer update laws for a versatile onlooker. The DC connect voltage is adaptively changed in relation to the PCC voltage to limit exchanging misfortunes in voltage source converter (VSC) and to stay away from its stumbling in delicate circulation networks. A feed-forward circle for PV commitment is incorporated to improve framework reaction under unique conditions. Reproduced and test outcomes portray the presentation of the GPV framework with previously mentioned functionalities. Improved consistent state and dynamic exhibitions are seen with the proposed nonlinear versatile assessment based control approach. The complete consonant twists (THDs) in lattice flows are discovered well inside the cut-off points recommended by an IEEE-519 norm..

Literature [4] presents Distribution Static Compensator (DSTATCOM) is proposed for pay of receptive force and unbalance brought about by different burdens in appropriation framework. An assessment of three distinct techniques is made to determine reference flows for a DSTATCOM. These strategies are a quick responsive force hypothesis, a coordinated reference outline hypothesis, and another Adaline-based calculation. The Adaline-based calculation is a versatile technique for removing reference current signs. These plans are mimicked under MATLAB climate utilizing SIMULINK and PSB tool stash. Reproduction and test results exhibit the presentation of these plans for the control of DSTATCOM..

Literature [5] In request to improve the nature of the force infused into a matrix, this paper presents a model prescient control procedure for three-stage four-leg lattice tied inverters. For the accommodation of improvement, the discrete-time model of the inverter in which obligation proportions are demonstrated as constant control factors is explored. A current following mistake arranged cost work is utilized as a basis to upgrade obligation proportions of the inverters. To wipe out the impacts of testing delay, a model

prescient control with postpone pay technique (MPC-DC) is proposed. Since there is a lot of figuring's in executing prescient control calculation, a twofold CPU, in particular FPGA in addition to DSP regulator is utilized to actualize equal estimation, in order to decrease the calculation time. Recreation and exploratory outcomes exhibit the adequacy of the proposed strategy.

Literature [6] depicts the model reference versatile control (MRAC) is proposed for a solitary stage shunt dynamic force channel (APF) to improve line power factor and to diminish line current sounds. The proposed APF regulator powers the stockpile current to be sinusoidal, with low current sounds, and to be in stage with the line voltage. The benefits of utilizing MRAC over ordinary relative basic control are its adaptability, flexibility, and strength; besides, MRAC can self-tune the regulator gains to guarantee framework security. Since the APF is a bilinear framework, it is difficult to plan the regulator. This paper will tackle the steadiness issue when a linearization technique is utilized to understand the nonlinearity of the framework. In addition, by utilizing Lyapunov's steadiness hypothesis and Barbalat's lemma, a versatile law is intended to ensure an asymptotic yield following of the framework..

Literature [7] during voltage plunges nonstop force conveyance from dispersed age frameworks to the matrix is alluring with the end goal of lattice upholds. To encourage the control of inverter-based dispersed force age adjusted to the normal difference in network necessities, summed up force control procedures dependent on symmetric-grouping parts are proposed in this paper, intending to control the conveyed quick force under lopsided voltage plunges. It is indicated that dynamic and receptive force can be autonomously controlled with two exclusively versatile boundaries. By changing these boundaries, the general amplitudes of swaying force can be easily managed, just as the pinnacle estimations of three-stage lattice flows. Thus, the force control of matrix intuitive inverters turns out to be very adaptable and versatile to different lattice necessities or plan imperatives. Moreover, two systems for synchronous dynamic and responsive force control are recommended that safeguard adaptable controllability; an application model is given to outline the straightforwardness and versatility of the proposed methodologies for online advancement control.

Literature [8] Voltage unbalance in a three-stage framework causes execution disintegration of PWM power converters by delivering 120 Hz voltage swells in the DC connect and by expanding the responsive force. To kill the DC interface voltage swell and the DC part of the responsive force, both positive-and negative-succession flows should

be controlled all the while, as per the paper by Rioual et al (1996). The creators utilized two coordinated reference outlines: a positive-arrangement current directed by a corresponding vital (PI) regulator in a positive simultaneous reference outline (SRF); and a negative-succession current managed by a PI regulator in a negative SRF. In the positive SRF, which pivots counter clockwise, the positive succession shows up as DC, while the negative arrangement shows up as 120 Hz. Interestingly, in the negative SRF, which pivots clockwise, the negative succession shows up as DC, while the positive arrangement shows up as 120 Hz

Literature [9] portrays the most recent couple of years, prohibitive matrix codes have emerged to guarantee the exhibition and strength of electrical organizations, which experience a huge combination of sustainable power sources and circulated age frameworks that are typically associated with the network through electronic force converters. In these codes, the infusion of positive-and negative-succession current segments gets important for satisfying, among others, the low-voltage ride-through necessities during adjusted and unequal matrix flaws. Notwithstanding, the presentation of traditional dq current regulators, applied to control converters, under unequal network voltage conditions is exceptionally inadequate, because of the unavoidable appearance of current motions. This paper dissects the presentation of the twofold simultaneous reference outline regulator and improves its structure by adding a decoupling network for assessing and repaying the unwanted current motions

Literature [10] Distributed age inverters have become a vital component to improve network proficiency and unwavering quality, especially during framework shortcomings. Under these extreme bothers, inverter-based force sources ought to achieve low-voltage ride-through prerequisites to continue taking care of the matrix and backing the framework voltage. Additionally, evaluated current can be needed to more readily use receptive force arrangements. This paper presents a reference generator able to achieve these two targets: to keep the infused flows inside wellbeing esteems and to process the force references for a superior use of the inverter power limit. The reference generator is completely adaptable since positive and negative dynamic and responsive forces can be all the while infused to improve ride-through administrations. Chosen exploratory outcomes are accounted for to assess the exhibition of the proposed reference generator under various control methodologies.

1.3 Problem Formation

The regulator [19] utilizes various relative thunderous (PR) regulators to accomplish singular stage current remuneration. The framework execution with PR regulators, is corrupted under variety of the framework recurrence as it gives limitless addition at the chose consonant frequencies. The non-ideal execution of endless additions could cause arrangement of flimsiness issues for pragmatic network interfaced DG frameworks [24]. Other than this, these methodologies [19]-[23] don't contribute for power quality improvement during nonlinear burdens and symphonious voltages in the framework. Besides, the zero-grouping and negative-arrangement powers are delivered by uneven flows with unequal voltages, which severely influence distinctive business loads and mechanical burdens associated at the higher finish of the circulation framework, for example, three-stage engine loads/high force loads. The ride through activity of network interfaced PV frameworks under low voltage droops, which guarantees the distinctive force quality functionalities of consonant current moderation, power factor revision, adjusting of lattice flows, dependable activity during anomalous/symphonious matrix voltages caused in appropriation framework, is rarely revealed in writing.

1.4 Objective Of The Project

This paper proposes an all-encompassing Kalman channel (EKF) based control technique for deficiency ride-through activity in two-stage framework associated photovoltaic (GPV) framework. In contrast to the regular regulators for ride-through activity, the proposed technique doesn't bargain with power quality improvement highlights in the framework while empowering ride-through activity. The regulator represents nonlinear burdens in the framework, matrix symphonious flows disposal and lattice flows adjusting in any event, during the consonant/misshaped network voltages. The IEEE standard-1547.4 urges the appropriated asset to ride-through during voltage aggravations brought about by shortcomings. For the ride-through activity, a breaking point is forced on PV dynamic force infusion to forestall inverter over-flows and DC-connect energy total, which decreases the lifetime of DC-interface capacitor. The responsive force is taken care of to the matrix, according to the profundity in voltage-droop. The de-evaluated PV cluster power is provided in situations where the inverter can't deal with the most extreme PV-power. The force quality improvement is guaranteed utilizing EKF state assessor, which unequivocally appraises the major burden flows. In dissemination network with present day nonlinear burdens, particularly at far outspread finishes, the framework

voltages are inclined to tremendous redirections and the proposed regulator gives a potential answer for look after dynamic/responsive force uphold and keep up force quality in the organization. The adequacy of the methodology is exhibited through re-enactment.

1.5 Organisation Of Project

- Chapter 1 gives an introduction to the concept
- Chapter 2 gives a description system configuration.
- Chapter 3 gives a description of control approach.
- Chapter 4 Introduction of Fuzzy logic controllers.
- Chapter 5 covers the simulation results by using PI controller and ANFIS controller.
- Chapter 6 summarizes and concludes the project work, and proposes recommendations for future work.

CHAPTER 2

SYSTEM CONFIGURATION

2.1 Introduction

2.1 Distributed generation

Distributed generation is electrical age and capacity performed by an assortment of little, lattice associated or circulation framework associated gadgets alluded to as disseminated energy assets (DER).

Customary force stations, for example, coal-terminated, gas, and atomic controlled plants, just as hydroelectric dams and huge scope sun oriented force stations, are incorporated and regularly require electric energy to be sent over significant distances. Paradoxically, DER frameworks are decentralized, particular, and more adaptable advancements that are found near the heap they serve, yet having limits of just 10 megawatts (MW) or less. These frameworks can include different age and capacity segments; in this occasion, they are alluded to as cross breed power frameworks.

DER systems ordinarily utilize sustainable power sources, including little hydro, biomass, biogas, sun oriented force, wind power, and geothermal force, and progressively assume a significant part for the electric force dissemination framework. A matrix associated gadget for power stockpiling can likewise be named a DER framework and is regularly called a dispersed energy stockpiling framework (DESS). By methods for an interface, DER frameworks can be overseen and facilitated inside a brilliant lattice. Disseminated age and capacity empowers the assortment of energy from numerous sources and may bring down natural effects and improve the security of supply.

Miniature matrices are present day, confined, little scope grids,[3][4] in opposition to the customary, incorporated power network (full scale framework). Miniature networks can detach from the brought together matrix and work independently, fortify framework versatility, and help moderate lattice unsettling influences. They are commonly low-voltage AC matrices, regularly use diesel generators, and are introduced by the network they serve. Miniature matrices progressively utilize a combination of various appropriated energy assets, for example, sun based cross breed power frameworks, which essentially decrease the measure of carbon produced..

Appropriated energy assets are mass-created, little, and less site-explicit. Their advancement emerged out of:

1. concerns over saw externalized expenses of focal plant age, especially natural concerns;;
 2. the expanding age, disintegration, and limit limitations upon T&D for mass power;
 3. the expanding relative economy of large scale manufacturing of more modest apparatuses over hefty assembling of bigger units and on location development;
- Along with higher relative costs for energy, higher by and large multifaceted nature and complete expenses for administrative oversight, duty organization, and metering and charging.

Capital business sectors have come to understand that right-sized assets, for singular clients, dissemination substations, or miniature lattices, can offer significant however mostly secret monetary preferences over focal plants. More modest units offered more prominent economies from large scale manufacturing than enormous ones could pick up through unit size. These expanded worth—because of enhancements in monetary danger, designing adaptability, security, and natural quality—of these assets can regularly more than counterbalance their obvious cost inconveniences. DG, versus focal plants, should be supported on a day to day existence cycle premise. Shockingly, a large number of the direct, and for all intents and purposes the entirety of the roundabout, advantages of DG are not caught inside customary utility income bookkeeping.

While the levelized cost of dispersed age (DG) is regularly more costly than customary, concentrated sources on a kilowatt-hour premise, this doesn't think about negative parts of traditional powers. The extra premium for DG is quickly declining as request increments and innovation advances and adequate and dependable interest may bring economies of scale, development, rivalry, and more adaptable financing that could make DG clean energy part of a more expanded future.

Disseminated age lessens the measure of energy lost in sending power on the grounds that the power is produced close to where it is utilized, maybe even in a similar structure. This additionally decreases the size and number of electrical cables that should be developed.

Commonplace DER frameworks in a feed-in levy (FIT) plot have low upkeep, low contamination and high efficiencies. Before, these attributes required devoted working architects and huge complex plants to lessen contamination. Be that as it may, current implanted frameworks can give these attributes robotized activity and sustainable

power, for example, sun based, wind and geothermal. This diminishes the size of intensity plant that can show a benefit.

Circulated energy asset (DER) frameworks are little scope power age or capacity innovations (ordinarily in the scope of 1 kW to 10,000 kW) used to give an option to or an upgrade of the conventional electric force framework. DER frameworks commonly are described by high introductory capital expenses per kilowatt. DER frameworks additionally fill in as capacity gadget and are regularly called Distributed energy stockpiling frameworks (DESS).

DER frameworks may incorporate the accompanying gadgets/advancements:

- Combined heat power (CHP), otherwise called cogeneration or recovery n
- Fuel cells
- Hybrid power systems (solar hybrid and wind hybrid systems)
- Micro combined heat and power (Microchips)
- Micro turbines
- Photovoltaic frameworks (ordinarily housetop sun based PV)
- Reciprocating motors
- Small wind power frameworks
- Sterling motor

Or on the other hand a mix of the above mentioned. For instance, half and half photovoltaic, CHP and battery frameworks can give full electric capacity to single family living arrangements without outrageous capacity costs.

2.11 Cogeneration

Dispersed cogeneration sources use steam turbines, flammable gas terminated energy units, miniature turbines or responding motors to turn generators. The hot fumes are then utilized for space or water warming, or to drive an absorptive chiller for cooling, for example, cooling. Notwithstanding flammable gas based plans, dispersed energy ventures can likewise incorporate other inexhaustible or low carbon powers including biofuels, biogas, landfill gas, sewage gas, coal bed methane, syngas and related oil gas.

Delta-ee experts expressed in 2013 that with 64% of worldwide deals, the energy component miniature joined warmth and force passed the traditional frameworks in deals in 2012. 20,000 units were sold in Japan in 2012 by and large inside the End Farm venture. With a Lifetime of around 60,000 hours for PEM power module units, which

shut down around evening time, this likens to an expected lifetime of somewhere in the range of ten and fifteen years. At a cost of \$22,600 before installation.[25] For 2013 a state sponsorship for 50,000 units is set up.

Moreover, liquid carbonate power module and strong oxide power modules utilizing gaseous petrol, for example, the ones from Fuel Cell Energy and the Bloom energy worker, or waste-to-energy cycles, for example, the Gate 5 Energy System are utilized as a disseminated energy asset.

2.12 Solar power

Photovoltaic, by a long shot the main sun oriented innovation for dispersed age of sun based force, utilizes sun powered cells amassed into sun based boards to change over daylight into power. It is a quickly developing innovation multiplying its overall introduced limit each couple of years. PV frameworks range from conveyed, private, and business housetop or building incorporated establishments, to enormous, brought together utility-scale photovoltaic force stations.

The dominating PV innovation is glasslike silicon, while flimsy film sun based cell innovation represents around 10% of worldwide photovoltaic organization. As of late, PV innovation has improved its daylight to power transformation proficiency, decreased the establishment cost per watt just as its energy compensation time (EPBT) and leveled cost of power (LCOE), and has arrived at matrix equality in any event 19 unique business sectors in 2014.

As most environmentally friendly power sources and dissimilar to coal and atomic, sun based PV is variable and non-dispatch capable, yet has no fuel costs, working contamination, just as extraordinarily diminished mining-wellbeing and working security issues. It produces top force around nearby early afternoon every day and its ability factor is around 20%.

2.13 Wind power

Wind turbines can be disseminated energy assets or they can be worked at utility scale. These have low upkeep and low contamination, yet appropriated wind not at all like utility-scale wind has a lot greater expenses than different wellsprings of energy. Likewise with sun powered, wind energy is variable and non-dispatch capable. Wind pinnacles and generators have considerable insurable liabilities brought about by high breezes, yet great working security. Dispersed age from wind half breed power frameworks joins wind power with other DER frameworks. One such model is the incorporation of wind turbines into sunlight based half breed power frameworks, as wind

will in general supplement sun based on the grounds that the pinnacle working occasions for every framework happen at various times and year

2.14 Hydro power

Hydroelectricity is the most generally utilized type of sustainable power and its latent capacity has just been investigated to a huge degree or is undermined because of issues, for example, natural effects on fisheries, and expanded interest for recreational access. Notwithstanding, utilizing current 21st century innovation, for example, wave power, can make a lot of new hydropower limit accessible, with minor ecological effect.

Particular and adaptable Next age dynamic energy turbines can be conveyed in exhibits to serve the requirements on a private, business, modern, city or even territorial scale. Miniature hydro active generators neither require dams nor impoundments, as they use the dynamic energy of water movement, either waves or stream. No development is required on the shoreline or ocean bed, which limits ecological effects on natural surroundings and disentangles the allowing cycle. Such force age additionally has insignificant ecological effect and non-conventional miniature hydro applications can be fastened to existing development, for example, docks, wharfs, connect projections, or comparable structures

2.15 Waste-to-energy

Civil strong waste (MSW) and normal waste, for example, sewage slop, food waste and creature excrement will deteriorate and release methane-containing gas that can be gathered and utilized as fuel in gas turbines or miniature turbines to deliver power as a dispersed energy asset. Furthermore, a California-based organization, Gate 5 Energy Partners, Inc. has built up a cycle that changes characteristic waste materials, for example, sewage slop, into biofuel that can be combusted to control a steam turbine that produces power. This force can be utilized in lieu of framework power at the waste source, (for example, a treatment plant, ranch or dairy).

2.16 Energy storage

2.16.1 Grid energy storage

A conveyed energy asset isn't restricted to the age of power however may likewise incorporate a gadget to store dispersed energy (DE). Distributed energy stockpiling frameworks (DESS) applications incorporate a few sorts of battery, siphoned hydro, compacted air, and warm energy stockpiling. Admittance to energy stockpiling for business applications is effectively available through projects, for example, energy stockpiling as an assistance (ESaaS).

2.16.2 PV storage

Regular battery-powered battery advancements utilized in the present PV frameworks incorporate, the valve controlled lead-corrosive battery (lead-corrosive battery), nickel-cadmium and lithium-particle batteries. Contrasted with different kinds, lead-corrosive batteries have a more limited lifetime and lower energy thickness. In any case, because of their high dependability, low self-release (4–6% every year) just as low venture and support costs, they are right now the overwhelming innovation utilized in little scope, private PV frameworks, as lithium-particle batteries are as yet being created and about 3.5 occasions as costly as lead-corrosive batteries. Besides, as capacity gadgets for PV frameworks are fixed, the lower energy and force thickness and in this way higher load of lead-corrosive batteries are not as basic concerning electric vehicles.

In any case, lithium-particle batteries, for example, the Tesla Power wall, can possibly supplant lead-corrosive batteries sooner rather than later, as they are as a rule seriously created and lower costs are relied upon because of economies of scale gave by enormous creation offices, for example, the Giga factory 1. Moreover, the Li-particle batteries of module electric vehicles may fill in as future stockpiling gadgets, since most vehicles are left a normal of 95 percent of the time, their batteries could be utilized to allow power to move from the vehicle to the electrical cables and back. Other battery-powered batteries that are considered for circulated PV frameworks incorporate, sodium-sulphur and vanadium redox batteries, two unmistakable sorts of a liquid salt and a stream battery, separately.

2.16.3 Vehicle-to-grid

People in the future of electric vehicles may be able to convey power from the battery in a vehicle-to-lattice into the network when required

An electric vehicle network can possibly fill in as a DESS.

2.16.4 Flywheels

A high level flywheel energy stockpiling (FES) stores the power produced from disseminated assets as precise motor energy by quickening a rotor (flywheel) to an extremely rapid of around 20,000 to more than 50,000 rpm in a vacuum nook. Flywheels can react rapidly as they store and input power into the matrix very quickly

2.2 Total Harmonic Distortion

The all out consonant mutilation, or THD, of a sign is an estimation of the symphonious bending present and is characterized as the proportion of the amount of the

forces of all symphonious parts to the intensity of the principal recurrence. THD is utilized to describe the linearity of sound frameworks and the force nature of electric force frameworks. Contortion factor is a firmly related term, once in a while utilized as an equivalent.

In sound frameworks, lower contortion implies the segments in an amplifier, enhancer or receiver or other hardware produce a more exact multiplication of a sound account.

In radio interchanges, lower THD implies unadulterated sign discharge without making impedances other electronic gadgets. Additionally, the issue of contorted and not eco-accommodating radio discharges seems, by all accounts, to be likewise significant with regards to range sharing and range detecting.

In force frameworks, lower THD implies decrease in pinnacle flows, warming, emanations, and centre misfortune in engines.

2.21 Definitions and Examples:

To comprehend a framework with information and a yield, for example, a sound enhancer, we start with an ideal framework where the exchange work is straight and time-invariant. At the point when a sign goes through a non-ideal, non-straight gadget, extra substance is added at the sounds of the first frequencies. THD is an estimation of the degree of that mutilation.

At the point when the principle execution model is the "purity" of the first sine wave (at the end of the day, the commitment of the first recurrence regarding its music), the estimation is most ordinarily characterized as the proportion of the RMS plentifulness of a bunch of higher consonant frequencies to the RMS sufficiency of the primary symphonious, or major, recurrence

$$\text{THD}_F = \frac{\sqrt{V_2^2 + V_3^2 + V_4^2 + \dots}}{V_1}$$

Where V_n is the RMS voltage of the n th symphonious and $n = 1$ is the major recurrence. By and by, the THDF is regularly utilized in sound bending determinations (rate THD); in any case, THD is a non-normalized detail and the outcomes between producers are not effectively practically identical. Since singular symphonious amplitudes are estimated, it is necessitated that the producer reveal the test signal recurrence reach, level and gain conditions, and number of estimations taken. It is conceivable to quantify the full 20–20

kHz range utilizing a scope (however mutilation for a central over 10 kHz is indistinct). For all sign handling hardware, aside from receiver preamplifiers, the favored addition setting is solidarity for mouthpiece preamplifiers, standard practice is to utilize most extreme increase. Estimations for ascertaining the THD are made at the yield of a gadget under determined conditions. The THD is typically communicated in percent or in dB comparative with the principal as contortion lessening.

A variation definition utilizes the essential in addition to sounds as the reference, however utilization is debilitate:

$$\text{THD}_R = \frac{\sqrt{V_2^2 + V_3^2 + V_4^2 + \dots}}{\sqrt{V_1^2 + V_2^2 + V_3^2 + \dots}} = \frac{\text{THD}_F}{\sqrt{1 + \text{THD}_F^2}}$$

These can be recognized as THDF (for "key"), and THDR (for "root mean square"). THDR can't surpass 100%. At low mutilation levels, the distinction between the two count strategies is unimportant. For example, a sign with THDF of 10% has a fundamentally the same as THDR of 9.95%. In any case, at higher twisting levels the error turns out to be huge. For example, a sign with THDF 266% has a THDR of 94%. An unadulterated square wave with limitless sounds has THDF of 48.3%, or THDR of 43.5%. Some utilize the expression "mutilation factor" as an equivalent word for THDR, while others use it as an equivalent word for THDF.

THD+N:

THD+N imply all out consonant twisting in addition to clamour. This estimation is considerably more typical and more equivalent between gadgets. It is normally estimated by contributing a sine wave, indent separating the yield, and contrasting the proportion between the yield signal with and without the sine wave:

$$\text{THD+N} = \frac{\sum_{n=2}^{\infty} \text{harmonics} + \text{noise}}{\text{fundamental}}$$

Like the THD estimation, this is a proportion of RMS amplitudes, and can be estimated as THDF (band passed or determined essential as the denominator) or, all the more generally, as THDR (complete contorted sign as the denominator). Sound Precision estimations are THDR, for example.

An important estimation should incorporate the data transmission of estimation. This estimation incorporates impacts from ground circle power line murmur, high-recurrence impedance, intermodulation contortion between these tones and the major, etc, notwithstanding symphonious bending. For psychoacoustic estimations, a weighting bend is applied, for example, A-weighting or ITU-R BS.468, which is planned to emphasize what is generally perceptible to the human ear, adding to a more exact estimation. For a given info recurrence and plentifulness, THD+N is complementary to SINAD, given that the two estimations are made over a similar transfer speed.

2.22 Measurement

The contortion of a waveform comparative with an unadulterated sine wave can be estimated either by utilizing a THD analyser to investigate the yield wave into its constituent music and taking note of the sufficiency of every comparative with the basic; or by counteracting the key with a step channel and estimating the leftover sign, which will be all out total symphonious twisting in addition to clamour.

Given a sine wave generator of exceptionally low intrinsic twisting, it tends to be utilized as contribution to enhancement gear, whose mutilation at various frequencies and sign levels can be estimated by inspecting the yield waveform.

There is electronic hardware both to create sine waves and to quantify mutilation; however a universally useful advanced PC furnished with a sound card can do consonant examination with reasonable programming. Distinctive programming can be utilized to create sine waves, yet the inborn mutilation might be excessively high for estimation of low-contortion enhancers.

Examples

For some standard signals, the above basis might be determined systematically in a shut structure. For instance, an unadulterated square wave has THDF equivalent to

$$\mathbf{THD_F} = \sqrt{\frac{\pi^2}{8} - 1} \approx \mathbf{0.483} = \mathbf{48.3\%}$$

The saw tooth signal possesses

$$\mathbf{THD_F} = \sqrt{\frac{\pi^2}{6} - 1} \approx \mathbf{0.803} = \mathbf{80.3\%}$$

The unadulterated even triangle wave has THDF of

$$\text{THD}_F = \sqrt{\frac{\pi^4}{96} - 1} \approx 0.121 = 12.1\%$$

For the rectangular heartbeat train with the obligation cycle μ (called at times the cyclic proportion), the THDF has the structure

$$\text{THD}_F(\mu) = \sqrt{\frac{\mu(1-\mu)\pi^2}{2\sin^2\pi\mu} - 1}, \quad 0 < \mu < 1$$

2.3 Phase locked loop (PLL)

The idea of Phase Locked Loops (PLL) first arose in the mid 1930's. But the innovation was not created as it now, the cost factor for building up this innovation was exceptionally high. Since the progression in the field of incorporated circuits, PLL has gotten one of the fundamental structure blocks in the gadgets innovation. In present, the PLL is accessible as a solitary IC in the SE/NE560 arrangement (560, 561, 562, 564, 565 and 567) to additionally diminish the purchasing cost, the discrete IC's are utilized to develop a PLL.

PLL applications

Frequency Modulation (FM) sound system decoders, FM Demodulation networks for FM activity.

- Frequency union that gives numerous of a reference signal recurrence.
- Used in motor speed controls, following channels.
- Used in recurrence move scratching (FSK) translates for demodulation transporter frequencies

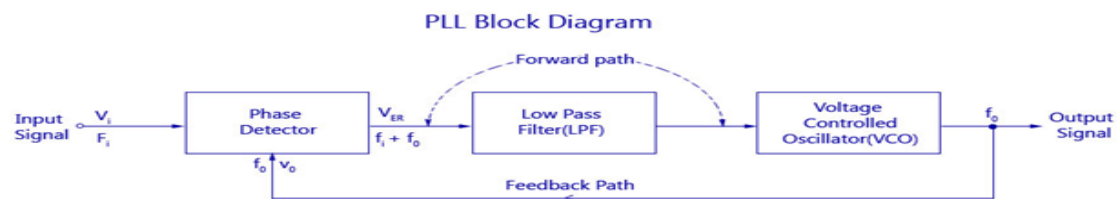


Fig2.1 Block Diagram of PLL

2.3.1 Phase Detector

This comparator circuit thinks about the information recurrence and the VCO yield recurrence and produces a dc voltage that is relative to the stage distinction between the two frequencies. The stage locator utilized in PLL might be of simple or computerized

type. Despite the fact that the greater part of the solid PLL incorporated circuits utilize simple stage locators, most of discrete stage finders are of the advanced kind. One of the most regularly utilized simple stage locator is the twofold adjusted blender circuit. A portion of the regular advanced sort stage identifiers are

2.3.2 Exclusive OR Phase Detector

A restrictive OR stage identifier is appeared in the figure beneath.



2.3.3 Exclusive-OR Phase Detector

It is acquired as a CMOS IC of type 4070. Both the frequencies are given as a contribution to the EX OR stage identifier. Complying with the EX-OR idea the yield turns out to be HIGH just if both of the data sources f_i or f_o turns out to be HIGH. Any remaining conditions will deliver a LOW yield. Allow us to consider a waveform where the info recurrence drives the yield recurrence by θ degrees. That is, f_i and f_o has a stage contrast of θ degrees. The dc yield voltage of the comparator will be an element of the stage distinction between its two information sources.

The figure shows the diagram of DC yield voltage as an element of the stage contrast among f_i and f_o . The yield DC voltage is most extreme when the stage identifier is 180° . This kind of stage locator is utilized when both f_i and f_o are square waves.

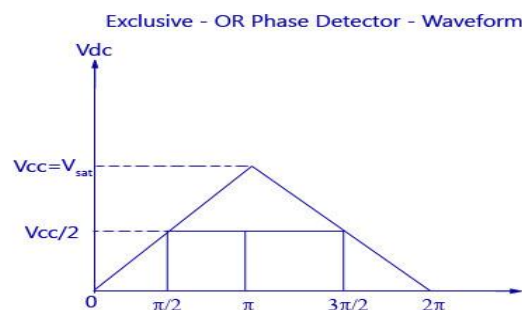


Fig 2.2 Exclusive-OR Phase Detector-Waveform

2.3.4 Edge Triggered Phase Detector

Edge set off stage finder is utilized when f_i and f_o are beat waveforms with under half obligation cycles. The figure of such a stage indicator utilizing a R-S Flip Flop is demonstrated as follows. Two NOR Gate (CD4001) are cross-coupled to shape a R-S Flip Flop. The yield of the stage locator changes its rationale state by setting off of the R-S Flip Flop. That is, the yield of the stage finder changes its rationale state on the positive edge of the info f_i and f_o . The benefit of such a finder can be perceived from the chart underneath. Obviously the DC yield voltage is straight over 360° .

2.3.5 Monolithic Phase Detectors

The solid kind stage identifier utilizes a CMOS type 4044 IC, which is profoundly preferred as the consonant affectability and obligation cycle issues are disregarded and the circuit will be react just to the change in the information signals. This is the most favoured stage locator in the basic applications as the stage blunder and the yield mistake voltage are free of varieties in the abundance and obligation patterns of the info waveforms.

2.3.6 Low Pass Filter (LPF)

A Low Pass Filter (LPF) is utilized in Phase Locked Loops (PLL) to dispose of the high recurrence parts in the yield of the stage finder. It likewise eliminates the high recurrence commotion. Every one of these highlights make the LPF a basic part in PLL and helps control the dynamic attributes of the entire circuit. The dynamic attributes incorporate catch and lock reaches, transfer speed, and transient reaction. The lock range is the following reach where the scope of frequencies of the PLL framework follows the adjustments in the info recurrence. The catch range is the reach wherein the Phase Locked Loops accomplishes the Phase Lock.

At the point when the channel transfer speed is decreased, the reaction time increments. But this lessens the catch range. In any case, it additionally helps in decreasing clamor and in keeping up the bolted circle through flashing misfortunes of sign. Two sorts of uninvolved channel are utilized for the LPF circuit in a PLL. An enhancer is utilized additionally with LPF to get pick up. The dynamic channel utilized in PLL is demonstrated as follows

2.3.7 Voltage Controlled Oscillator (VCO)

The primary capacity of the VCO is to produce a yield recurrence that is straightforwardly relative to the information voltage. The association chart of a SE/NE

566 VCO is appeared in the figure beneath. The greatest recurrence of the VCO is 500 KHz.

This VCO gives concurrent square wave and three-sided wave yields as an element of the info voltage. The recurrence of wavering is controlled by the resistor R and capacitor C alongside the voltage V_c applied to the control terminal.

2.3.8 PLL working

Allow us to believe the free running recurrence to be f_r . Leave f_r alone the recurrence at which the Voltage Controlled Oscillator (VCO) is running without input signal. Let the information signal f_i that is expanding from zero be applied to the stage comparator.

A chart between the blunder voltage and info recurrence is demonstrated as follows. It very well may be seen that when the information recurrence is lesser than f_{i1} , the blunder voltage V_e is diminished to zero. Right now the VCO will work at the free running recurrence, f_r . At the point when the information recurrence, f_i increments and spans f_{i1} , the mistake voltage bounces from zero to a negative voltage. This worth will be equivalent to the contrast between the info recurrence and real VCO yield recurrence ($f_i - f_o$). This coming about mistake voltage is then handled by separating, intensifying, and applying the enhanced voltage V_d to the control terminals of the VCO.

The immediate recurrence of VCO diminishes on the grounds that f_o succumbs to negative estimations of V_d and increments for positive estimations of V_{rf} . At some moment of time, the diminishing recurrence of the VCO approaches f_{i1} (lower edge of the catch range), at that point lock results-in, and the yield signal recurrence of the VCO might be equivalent to the info signal recurrence (that is, $f_o = f_i$). The VCO recurrence locks with input signal recurrence up to f_{i2} (the upper finish of the lock range). On the off chance that the information signal recurrence surpasses f_{i2} , at that point blunder voltage V_g will tumble to zero and the VCO will work at the free running recurrence f_r , as shown in figure.

In the event that the info signal recurrence is currently gradually cleared back and it achieves the estimation of f_{d1} then the circle (VCO recurrence) locks with the information signal recurrence, causing a positive bounce of the mistake voltage V_e . So the VCO yield recurrence increments from f_r ceaselessly till f_o gets equivalent to f_i . The VCO recurrence f_o locks with the info signal recurrence f_i upto f_{d2} (the lower edge of the lock range) as appeared in figure by dabbed lines. Presently in the event that the

recurrence of the information signal falls beneath fd2, at that point the blunder voltage V_{er} will tumble to zero and the VCO will work at the free running recurrence.

Advanced stage bolted circles establish a significant square in correspondence circuits. They are utilized to recuperate the clock sign of the sent sign at the collector end, consequently give information synchronization at the two sides of correspondence circuits.

The square graph of a PLL is appeared in fig. 2.3. 'Information in' is the reference signal, which is either the gotten signal or the yield of a nearby oscillator. The periods of the reference signal and the progressively revised clock are looked at the stage finder (PD), where a high yield signal is delivered related to the stage distinction of the info waveforms. The subsequent sign is gone through a circle channel, which is a low-pass channel used to add a post to the general framework. The presentation of an additional post notwithstanding the one presented by the voltage-controlled oscillator (VCO) is important to the furthest limit of dealing with the input circle, subsequently forestalling the locking of the yield waveform on higher sounds of the reference clock. VCO changes the stage data into genuine clock flags whose swaying recurrence is controlled through the voltage yield of the PD subsequent to being arrived at the midpoint of by the circle channel. The motions at the yield of the VCO are taken care of back to the PD after a predetermined number of cycles, N . This number is set through the counter and controls the increase factor over the reference clock that the yield signal is bolted onto. The shut circle gain of the PLL can be assessed utilizing the increases of the individual sub-blocks:

Phase detector: K_{PD}

$$K_F = \frac{K_{LPF}}{1 + \frac{s}{p}}$$

Loop filter:

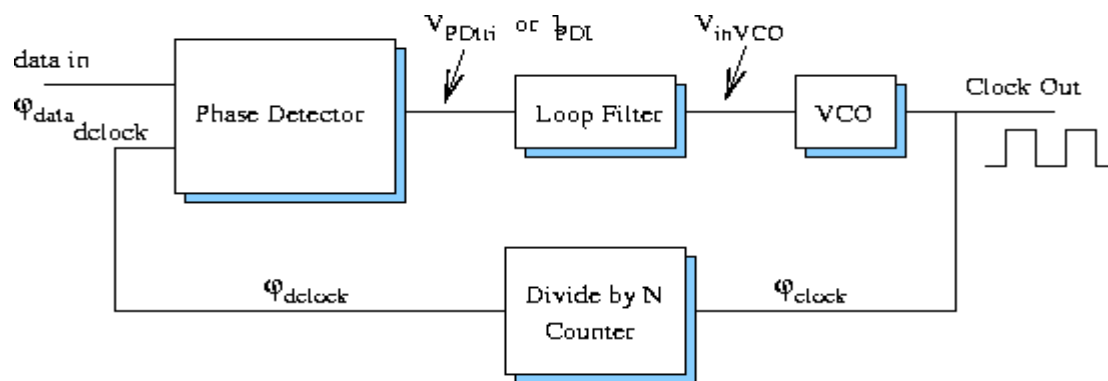


Fig 2.3: Block Diagram of a PLL

$$\triangleright \text{VCO: } \frac{K_{VCO}}{s}$$

The overall closed loop gain becomes:
$$H(s) = \frac{\Phi_{clock}}{\Phi_{data}} = \frac{K_{PD}K_{VCO}K_F}{s + \frac{1}{N}K_{PD}K_{VCO}K_F}$$

This is a subsequent request move work because of the s terms presented by the VCO and the circle channel. Hypothetically, a first request PLL, without a circle channel, can likewise work. Be that as it may, as it was called attention to, the second request framework is simpler to control and would permit following of quick varieties in the time area, in this manner keeping the framework from locking onto higher sounds of the reference signal.

2.4 EKF

In assessment hypothesis, the all-encompassing Kalman channel (EKF) is the nonlinear variant of the Kalman channel which linearizes about a gauge of the current mean and covariance. On account of all around characterized change models, the EKF has been considered the de calculate standard the hypothesis of nonlinear state assessment, route frameworks and GPS the Kalman channel is the ideal straight assessor for direct framework models with added substance free background noise both the progress and the estimation frameworks. Sadly, in designing, most frameworks are nonlinear, so endeavours were made to apply this sifting technique to nonlinear frameworks; Most of this work was done at NASA. The EKF adjusted procedures from analytics, in particular multivariate Taylor arrangement extensions, to linearize a model about a working point. In the event that the framework model (as depicted underneath) isn't notable or is off base, at that point Monte Carlo strategies, particularly molecule channel, are utilized for assessment. Monte Carlo methods originate before the presence of the EKF yet are all the more computationally costly for any tolerably dimensioned state-space.

In the all-inclusive Kalman channel, the state progress and perception models don't should be straight elements of the state however may rather be differentiable capacities.

Here w_k and v_k are the cycle and perception commotions which are both thought to be zero mean multivariate Gaussian clamours with covariance Q_k and R_k individually. u_k is the control vector.

$$\begin{aligned}\mathbf{x}_k &= f(\mathbf{x}_{k-1}, \mathbf{u}_k) + \mathbf{w}_k \\ \mathbf{z}_k &= h(\mathbf{x}_k) + \mathbf{v}_k\end{aligned}$$

The capacity f can be utilized to process the anticipated state from the past gauge and likewise the capacity h can be utilized to register the anticipated estimation from the anticipated state. Nonetheless, f and h can't be applied to the covariance straightforwardly. Rather a lattice of fractional subsidiaries (the Jacobian) is figured.

At each time step, the Jacobian is assessed with current anticipated states. These networks can be utilized in the Kalman channel conditions. This cycle basically linearizes the non-direct capacity around the current gauge.

See the Kalman Filter article for notational comments. Discrete _time anticipate and update condition

Notation $\hat{\mathbf{x}}_{n|m}$ represents the estimate of \mathbf{x} at time n given observations up to and including at time $m \leq n$.

Predicted state estimate

$$\hat{\mathbf{x}}_{k|k-1} = f(\hat{\mathbf{x}}_{k-1|k-1}, \mathbf{u}_k)$$

Predicted covariance estimate

$$\mathbf{P}_{k|k-1} = \mathbf{F}_k \mathbf{P}_{k-1|k-1} \mathbf{F}_k^\top + \mathbf{Q}_k$$

2.5 Boost Converter:

A lift converter (venture up converter) is a DC-to-DC power converter that means up voltage (while venturing down current) from its information (supply) to its yield (load). It is a class of exchanged mode power supply (SMPS) containing in any event two semiconductors (a diode and a semiconductor) and at any rate one energy stockpiling component: a capacitor, inductor, or the two in blend. To diminish voltage swell, channels made of capacitors (at times in mix with inductors) are ordinarily added to quite a converter's yield (load-side channel) and information (supply-side channel).

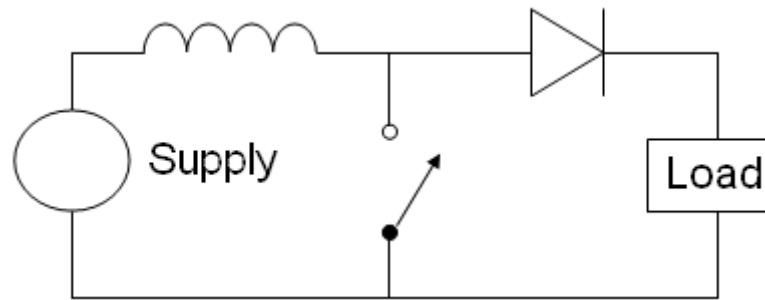
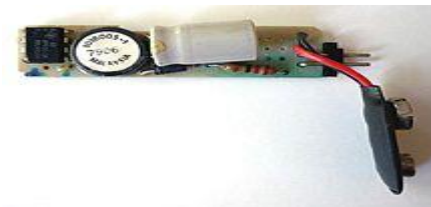


Fig 2.4 The basic schematic of a boost converter.

The switch is typically a MOSFET, IGBT, or BJT.

Force for the lift converter can emerge out of any appropriate DC sources, for example, batteries, sun powered boards, rectifiers and DC generators. A cycle that transforms one DC voltage to an alternate DC voltage is called DC to DC transformation. A lift converter is a DC to DC converter with a yield voltage more noteworthy than the source voltage. A lift converter is once in a while rung a stage converter since it "ventures up" the source voltage. Since power ($p=vi$) should be preserved, the yield current is lower than the source current.

Applications



Boost converter from a TI calculator, generating 9 V from 2.4 V provided by two AA rechargeable cells.

Battery power frameworks regularly stack cells in arrangement to accomplish higher voltage. In any case, adequate stacking of cells is preposterous in numerous high voltage applications because of absence of room. Lift converters can build the voltage and decrease the quantity of cells. Two battery-controlled applications that utilization support converters are utilized in half breed electric vehicles (HEV) and lighting frameworks.

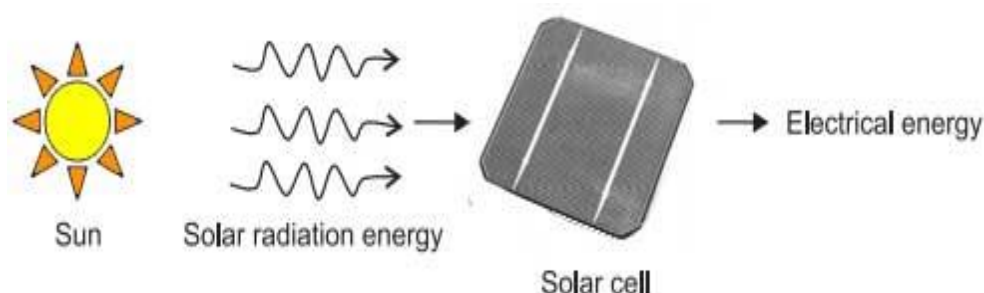
The NHW20 model Toyota Prius HEV utilizes a 500 V engine. Without a lift converter, the Prius would require almost 417 cells to control the engine. Notwithstanding, a Prius really utilizes just 168 cells and lifts the battery voltage from 202 V to 500 V. Lift converters additionally power gadgets at more modest scope applications, for example, versatile lighting frameworks. A white LED regularly requires

3.3 V to transmit light, and a lift converter can venture up the voltage from a solitary 1.5 V soluble cell to control the light.

An unregulated lift converter is utilized as the voltage increment system in the circuit known as the 'Joule criminal'. This circuit geography is utilized with low force battery applications, and is focused on the capacity of a lift converter to 'take' the leftover energy in a battery. This energy would somehow or another be squandered since the low voltage of an almost exhausted battery makes it unusable for an ordinary burden. This energy would somehow stay undiscovered on the grounds that numerous applications don't permit enough current to move through a heap when voltage diminishes. This voltage decline happens as batteries become exhausted, and is a quality of the universal antacid battery. Since the condition for power is ($p=v^2 r$), and R will in general be steady, power accessible to the heap goes down essentially as voltage diminishes..

2.6 Solar power generation:

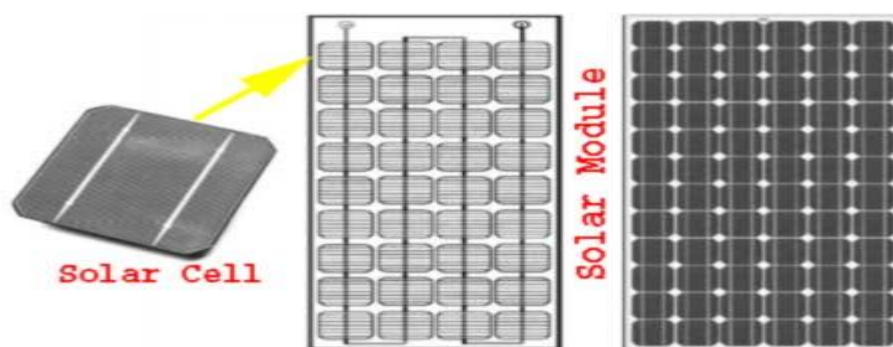
At the point when daylight strikes on photovoltaic sun oriented boards sun powered power is created. That is the reason this is additionally alluded to as photovoltaic sun oriented, or PV sunlight based.



2.6.1 Principles of Solar Electricity

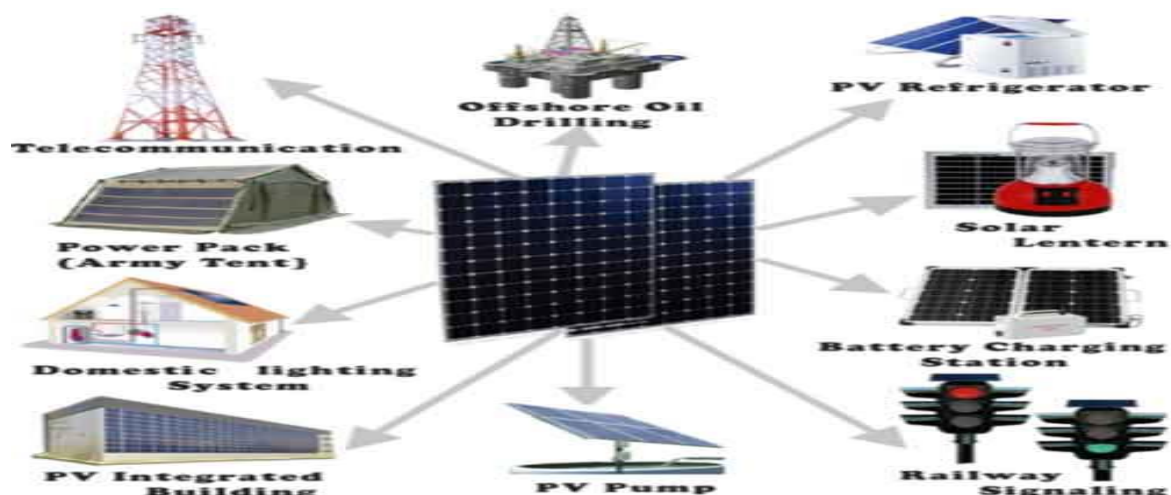
Age of power by utilizing sun oriented energy relies on the photovoltaic impact in some particular materials. There are sure materials that produce electric flow when these are presented to coordinate daylight. This impact is found in blend of two slender layers of semiconductor materials. One layer of this blend will have an exhausted number of electrons. At the point when daylight strikes on this layer it assimilates the photons of daylight beam and therefore the electrons are energized and leap to the next layer. This wonder makes a charge distinction between the layers and coming about to a small likely contrast between them. The unit of such mix of two layers of semiconductor materials for delivering electric likely distinction in daylight is called sun based cell. Silicon is regularly utilized as the semiconductor material for delivering such sun oriented

cell. For building cell silicon material is cut into slender wafers. A portion of these wafers are doped with pollutions. At that point the un-doped a lot wafers are then sandwiched together to fabricate sun powered cell. Metallic strip is then connected to two outrageous layers to gather current. Conductive metal strips connected to the cells take the electrical flow. One sun oriented cell or photovoltaic cell isn't equipped for creating wanted power rather it delivers extremely little measure of power henceforth for removing wanted degree of power wanted number of such cells are associated together in both equal and arrangement to shape a sun based module or photovoltaic module.



2.6.2 Application of Solar Electricity

Sun based electric force age framework is valuable for delivering moderate measure of intensity. The framework fills in as long as there is a decent force of normal daylight. Where sun based modules are introduced should be liberated from hindrances, for example, trees and structures in any case there will be shade on the sun oriented board which influences the presentation of the framework. It is an overall view that sun based power is an unrealistic option of ordinary wellspring of power and should be utilized when there is no customary option of traditional wellspring of power accessible. Be that as it may, this isn't the genuine case. Regularly it is appear to be that sun based power is more cash sparing option than other customary choices of traditional power.



It is consistently prudent to introduce a sunlight based light or a sun oriented force source where it is troublesome and expensive to get point from nearby electric stockpile authority, for example, in far off nursery, shed or carport where standard electric inventory point isn't accessible. Sun based power framework is more dependable and continuous as it doesn't experience the ill effects of undesirable force cut from electric inventory organization. For developing a versatile electric force source, for moderate force prerequisites sunlight based module is acceptable decision. It very well may be valuable while outdoors, dealing with outside destinations. It is best methods for making efficient power energy for our own motivation and might be for offering overflow energy to clients however for delivering power in business scale the speculation and volume of the framework turns out to be enormous enough. All things considered region of the task will be a lot bigger than regular one. Despite the fact that for running not many lights and low-power electrical devices, for example, PC, measured TV, small cooler and so forth sun based power framework is very appropriate given there is adequate free space on ground or on rooftop top for introducing sunlight based boards. In any case, it isn't at all practical to run high-control burning-through electric types of gear like fast fans, radiators, clothes washers, forced air systems and force devices with the assistance of sun oriented power as the expense of creation such high energy is very higher that it is normal. Besides there might be absence of room accessibility in your premises for establishment of huge sunlight based board. Ideal employments of ease sun based boards are charging batteries in processions and recreational vehicles or on boats when these are not in development given there should be tickle charging office from dynamo during development of these vehicles.

Types of Solar Power Station

There are mainly four types of solar power stations.

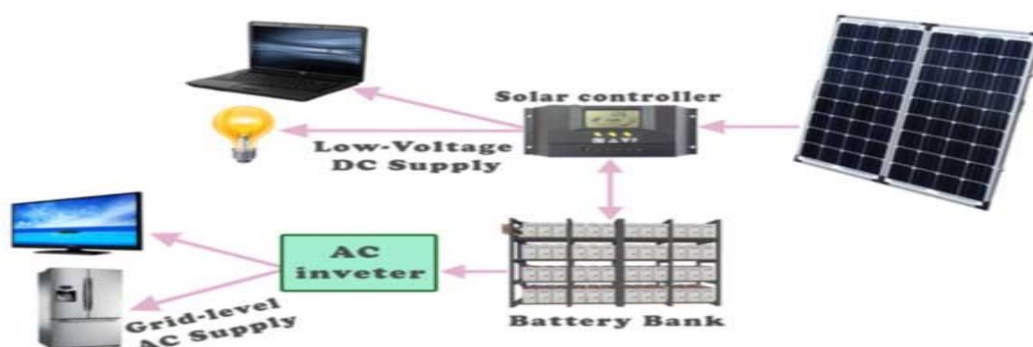
1. Stand Alone or Off Grid type Solar Power Plant
2. Grid Tie type Solar Power Plant
3. Grid Tie with Power Backup or Grid Interactive type Solar Power Plant
4. Grid Fullback type Solar Power Plant.

Let us discuss a brief introduction of each type of solar power plant.

2.6.3 Stand Alone or Off Grid Solar Power Station

This is most generally utilized photovoltaic establishment used to give limited power without customary wellspring of electric force at certain area. As the name

favours this framework doesn't keep any immediate or aberrant association with any lattice type organization. In independent framework the sun oriented modules produce electric energy which is used to charge a capacity battery and this battery conveys power to the associated load. Independent frameworks are typically little framework with under 1 kilo watt age limit.

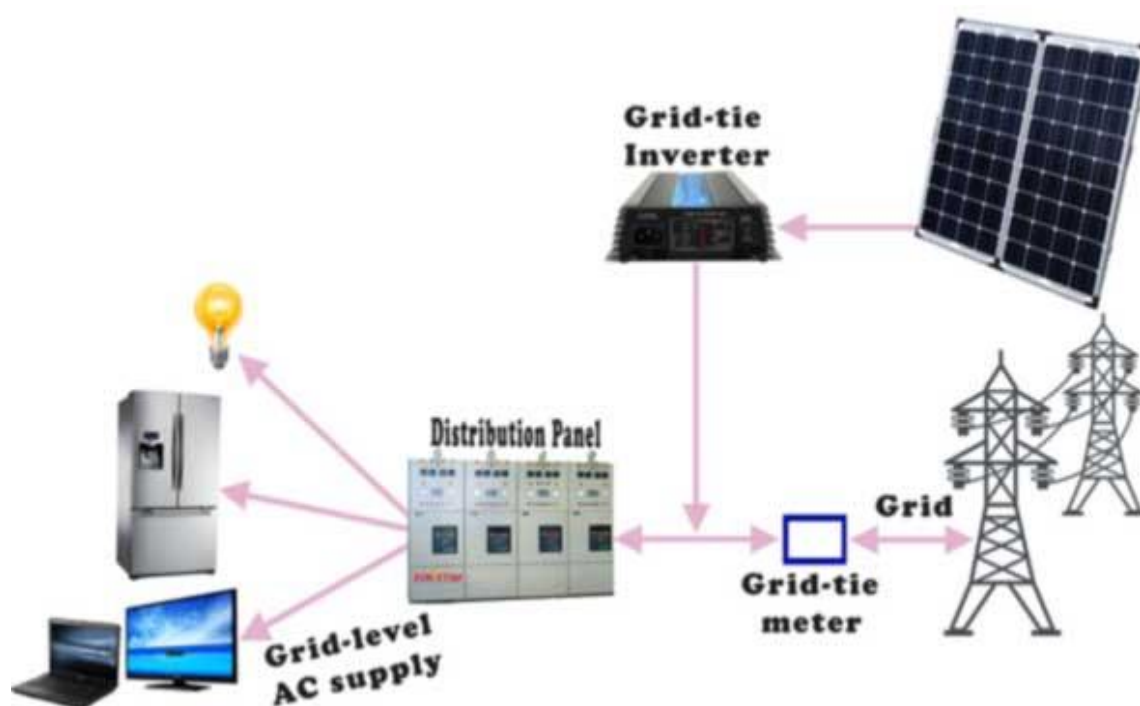


2.6.4 Grid Tie Solar Power Station

In certain nations office is accessible of offering capacity to the nearby or public framework. This is picking up prevalence in Europe and the United States. This framework encourages both electric service organizations just as the shoppers. Here purchasers can produce power by their own plant and can offer the excess to the power service organization through matrix associated with their plant. As the buyers sell the influence they can bring in cash as return of their speculation for establishment of hostage power plant then again electric service organizations can lessen their capital venture on their own plant for power age. In a matrix tie nearby planetary group, purchasers burn-through power delivered by sun based hostage power plant during bright day time and furthermore trade overflow energy to network however around evening time while sunlight based plant doesn't create energy, they import electric energy from framework for utilization. The fundamental burden of this framework is that if there is a force cut in the lattice, the sun based modules should be disengaged from the matrix. This framework isn't in every case entirely productive particularly where generally speaking most extreme interest of the framework doesn't happen at the pinnacle bright time of the day. In hot atmosphere where the force interest for cooling machines gets greatest during top radiant time of the day, this lattice tie sun oriented force age framework works most proficiently.

Lattice tie galaxies are of two kinds one with single full scale focal inverter and other with various miniature inverters. In the previous kind of close planetary system, the sun based boards just as framework supply are associated with a typical focal inverter

called network tie inverter as demonstrated as follows. The inverter here believes the DC of the sunlight based board to framework level AC and afterward feeds to the network just as the buyer's conveyance board contingent on the moment interest of the frameworks. Here framework tie inverter likewise screens the force being provided from the lattice. On the off chance that it finds any force cut in the matrix, it incites exchanging arrangement of the nearby planetary group to detach it from the network to guarantee no sun based power can be taken care of back to the framework during power cut. There is on energy meter associated in the principle framework supply line to record the energy fare to the network and energy import from the lattice.



As we previously told there is another sort of lattice tie framework where different miniature inverters are utilized. Here one miniature inverter is associated for every individual sun powered module. The essential square outline of this framework is fundamentally the same as past one aside from the miniature inverters are associated together to deliver wanted high AC voltage. In past case the low immediate voltage of sun oriented boards is first changed over to exchanging voltage then it is changed to high rotating voltage by change activity in the inverter itself yet for this situation the individual substituting yield voltage of miniature inverters are added together to deliver high rotating voltage.



2.6.5 Grid Tie with Power Backup Solar Power Generation

It is likewise called matrix intelligent framework. This is a mix of a framework tie sun oriented force age unit and capacity battery bank. As we stated, the primary downside of framework tie framework is that when there is any force cut in the network the sun powered module is disengaged from the framework. For maintaining a strategic distance from intermittence of supply during power cut period one battery bank of adequate limit can be associated with the framework as force reinforcement.

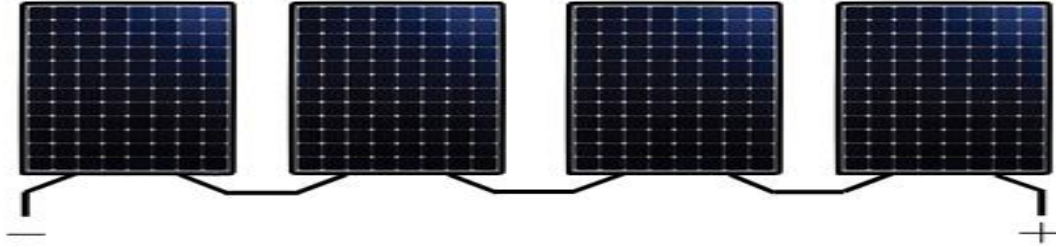
2.6.6 Grid fall-back Solar Power Generation

Network fall-back is generally solid and stable framework essentially utilized for charging more modest families. Here sunlight based modules charge a battery bank which thusly supplies dispersion sheets through an inverter. At the point when the batteries are released to a pre-indicated level, the framework naturally switches back to the lattice power supply. The sun oriented modules at that point revive the batteries and after the batteries are being energized to a pre – determined level again the framework switches back to sun based force. We don't sell power back to the power service organizations through this framework. All the force that we produce is used for ourselves as it were.

Solar Panels

The fundamental piece of a sun powered electric framework is the sun based board. There are different sorts of sun based board accessible on the lookout. Sun oriented boards are otherwise called photovoltaic sun powered boards. Sun oriented board or sun based module is essentially a variety of arrangement and equal associated sun powered cells. The potential contrast created across a sunlight based cell is about 0.5 volt and

consequently wanted number of such cells to be associated in arrangement to accomplish 14 to 18 volts to charge a standard battery of 12 volts. Sun based boards are associated together to make a sun powered exhibit. Numerous boards are associated together both in equal and arrangement to accomplish higher current and higher voltage individually.



Above fig shows the design of a twofold stage matrix interfaced sun powered photovoltaic framework with neighbourhood loads associated at PCC (Point of Common Coupling). The framework incorporates a PV exhibit, three-stage voltage source inverter (VSI), the lift converter, interfacing inductors, DC connect capacitor, swell channel and the straight/nonlinear burdens. The demonstrating philosophy for PV exhibit is accounted for in the writing [27]. A two-stage framework is considered here, where the DC-DC help converter guarantees the greatest force extraction from the PV cluster, utilizing steady conductance (InC) [28] based most extreme force extraction strategy, due the focal points it offers [28], disregarding a couple of negative marks [28]. In InC calculation, the bearing of bother to arrive at most extreme force point is chosen by the contrast between the steady conductance and the conductance offered by the PV cluster.

2.7 System configuration

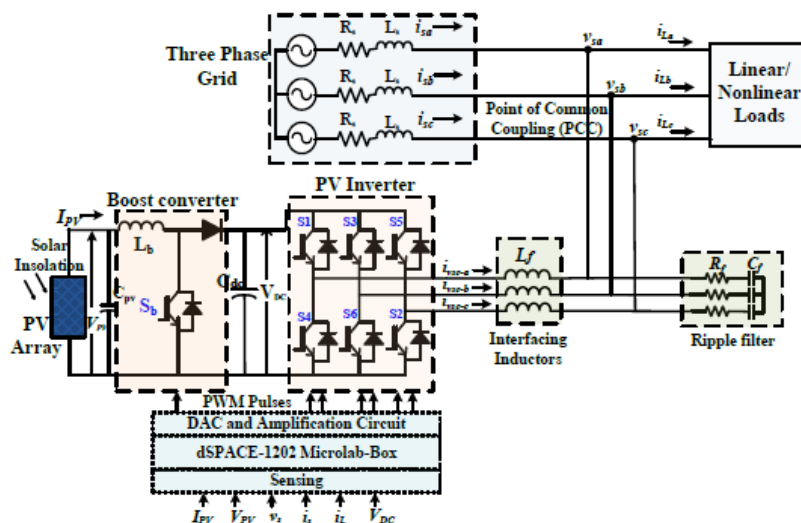


Fig.2.5. Configuration of two stage grid interfaced PV system

Notwithstanding, under serious lattice side blames, the PV cluster are made to work under non-MPPT mode, as the PV inverter can't deal with the most extreme PV power. The waves in the network flows are killed utilizing interfacing inductors and the VSI exchanging commotions are consumed by the wave channel. The plan and displaying technique of the framework, is as introduced in [2]. The subtleties of framework boundaries are accounted for in Appendix.

CHAPTER 3

CONTROL APPROACH

The precise control for the network interfaced power converter and the lift converter, are depicted here. The fundamental contributions to the PV inverter, are network flows (isa, isb, isc), load currents (iLa, iLb, iLc), PCC voltages (vsa, vsb, vsc) and the DC interface voltage (VDC); while the lift converter regulator principally requires PV-cluster voltage (VPV) and current (IPV) as its sources of info. The reference matrix flows are assessed utilizing the control plot and the hysteresis regulator is utilized to guarantee that the detected network flows follow the reference framework flows. The general control schematic for PV inverter is portrayed in Fig. 3.1. The various targets of the control are exhibited by division of control into five modules in particular, (I) load flows handling through EKF plot, (ii) appointing the heap current loads, (iii) assessment of misfortune segment and the PV feed forward segment, (iv) Fault ride through control, and (v) age of inverter gating beats. These are clarified as follows.

A. EKF Scheme for Load Currents Processing

The EKF plot for assessment of principal segments of burden current, is portrayed here. The KF is numerical technique, which works through forecast and amendment component. It is a recursive structure permits its constant execution without putting away perceptions or past evaluations. It gives data about the nature of the assessment by giving, notwithstanding the best gauge, the fluctuation of the assessment error. The KF can address itself and exploits revisions between obscure elements and update itself. Generally, the KF calculation predicts another state from its past assessment by adding a revision term relative to anticipated mistake. Thusly, this blunder is factually limited. Initially, the load current, is expressed as,

$$i_{La} = \sum_n I_{Lan} \cos(\omega_n t + \phi_n) \dots (1)$$

In which i_{pn}, ϕ_n, ω_n are adequacy, stage and recurrence of the nth symphonious segment. The heap current at kth testing moment (y_k), is communicated as,

$$y_k = I_{La1} \cos(K\omega_1 T_s + \phi_n) + \varepsilon_k \dots (2)$$

Where, ' T_s ' is the examining time and ε_k is Gaussian clamor with zero mean and variance σ^2 . The articulation (2) is expressed as far as assessed key burden current (\hat{y}_k) as,

$$y_k = \hat{y}_k + \varepsilon_k \dots (3)$$

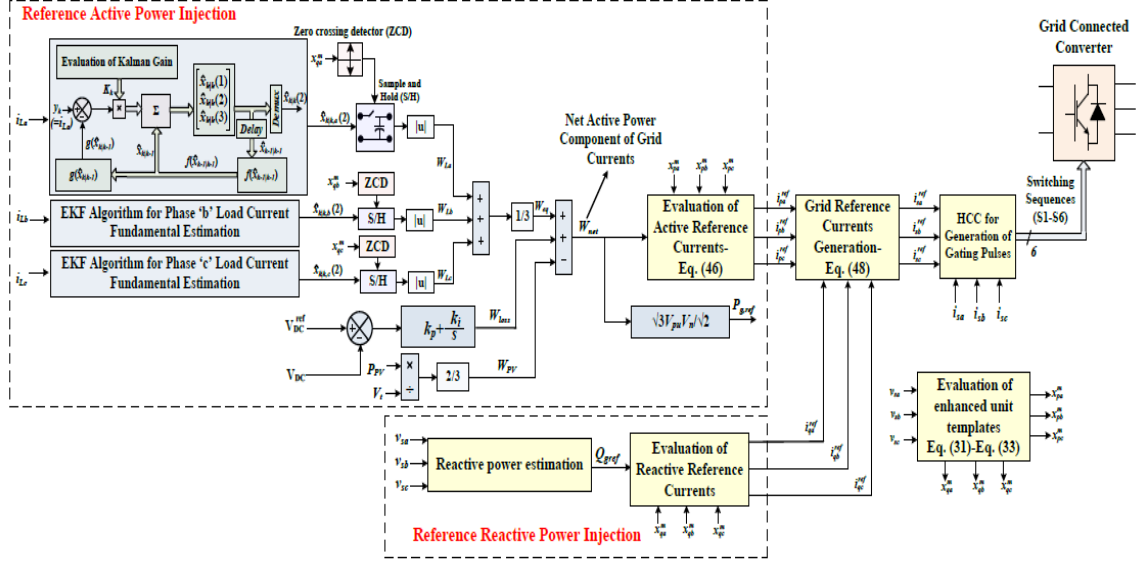


Fig.3.1 Control schematic for age of PV rearranges gating beats

in the wake of considering three back to back examples of burden flows at examining time T_s , the single sinusoid, ' fulfils the accompanying relationship, $\widehat{\mathbf{y}}_k$

$$\widehat{\mathbf{y}}_k - 2 \cos K \omega T_s \widehat{\mathbf{y}}_{k-1} + \widehat{\mathbf{y}}_{k-2} = \mathbf{0} \quad \text{--- (4)}$$

The assessed state-space vector at $(k-1)$ th moment is characterized as,

$$\widehat{\mathbf{x}}_{k-1/k-1} = [2 \cos(k-1) \omega T_s \quad \widehat{\mathbf{y}}_{k-1} \quad \widehat{\mathbf{y}}_{k-2}]^T \quad \text{--- (5)}$$

The comparing signal at k th moment can be distinguished as,

$$\widehat{\mathbf{x}}_{k/k-1} = \begin{bmatrix} 1 & 0 & 0 \\ 0 & 2 \cos K \omega T_s & -1 \\ 0 & 1 & 0 \end{bmatrix} \widehat{\mathbf{x}}_{k-1/k-1} \quad \text{--- (6)}$$

The $\widehat{\mathbf{x}}_{k-1/k-1}$ represents the estimated state variable at $(k-1)$ th instant with given values at $(k-1)$ th instant; and ' $\widehat{\mathbf{x}}_{k/k-1}$ ' represents the estimated state variable at k th instant with given values at $(k-1)$ th instant. Thus, from (4)-(6), (3) can be expressed as,

$$\mathbf{y}_k = [0 \quad 2 \cos K \omega T_s \quad -1] \widehat{\mathbf{x}}_{k/k-1} + \boldsymbol{\varepsilon}_k \quad \text{--- (7)}$$

Nonlinear equations (6)-(7), are formulated as,

$$\widehat{\mathbf{x}}_{k/k-1} = \mathbf{f}(\widehat{\mathbf{x}}_{k-1/k-1}) \text{ and } \mathbf{y}_k = \mathbf{g}(\widehat{\mathbf{x}}_{k/k-1}) + \boldsymbol{\varepsilon}_k \quad \text{--- (8)}$$

Where,

$$\mathbf{f}(\widehat{\mathbf{x}}_{k-1/k-1}) = \begin{bmatrix} 1 & 0 & 0 \\ 0 & 2 \cos K \omega T_s & -1 \\ 0 & 1 & 0 \end{bmatrix} \widehat{\mathbf{x}}_{k-1/k-1} \quad \text{--- (9)}$$

$$\widehat{\mathbf{y}}_k = \mathbf{g}(\widehat{\mathbf{x}}_{k/k-1}) = [0 \quad 2 \cos K \omega T_s \quad -1] \widehat{\mathbf{x}}_{k/k-1} \quad \text{--- (10)}$$

The nonlinear recursive channel is applied to appraise the greatness of the sign and its recurrence significantly under presence of the commotion, by linearizing the framework (8)- (10) as,

$$\hat{\mathbf{x}}_{k/k-1} = \mathbf{f}(\hat{\mathbf{x}}_{k-1/k-1}) \text{ --- (11)}$$

$$\hat{\mathbf{x}}_{k/k} = \hat{\mathbf{x}}_{k/k-1} + \mathbf{K}_k(\mathbf{y}_k - \mathbf{g}(\hat{\mathbf{x}}_{k/k-1})) \text{ --- (12)}$$

Hence the assessed state vector $\hat{\mathbf{x}}_{k/k}$ from (12), assessed for kth moment, is applied to framework. The Kalman pick up (\mathbf{K}_k) in (12) is assessed as,

$$\begin{aligned} \mathbf{K}_k &= \hat{\mathbf{P}}_{k/k-1} \frac{\partial \mathbf{g}^T}{\partial \hat{\mathbf{x}}} | (k/k) \\ &- 1) [\hat{\mathbf{P}}_{k/k-1} \frac{\partial \mathbf{g}}{\partial \hat{\mathbf{x}}} | (k/k-1) \hat{\mathbf{P}}_{k/k-1} \frac{\partial \mathbf{g}^T}{\partial \hat{\mathbf{x}}} | (k/k-1) + \mathbf{R}_0]^{-1} \text{ ---} \\ &- (13) \end{aligned}$$

The error covariance vector $\hat{\mathbf{P}}_{k/k-1}$ is evaluated and updated as follows.

$$\hat{\mathbf{P}}_{k/k-1} = \frac{\partial \mathbf{f}}{\partial \hat{\mathbf{x}}} | (k/k-1) \hat{\mathbf{P}}_{k-1/k-1} \frac{\partial \mathbf{f}^T}{\partial \hat{\mathbf{x}}} | (k/k-1) + \mathbf{Q}_0 \text{ --- (14)}$$

$$\hat{\mathbf{P}}_{k/k} = \hat{\mathbf{P}}_{k/k-1} - \mathbf{K}_k \frac{\partial \mathbf{g}}{\partial \hat{\mathbf{x}}} | (k/k-1) \hat{\mathbf{P}}_{k/k-1} \text{ --- (15)}$$

$$\frac{\partial \mathbf{f}}{\partial \hat{\mathbf{x}}} | (\mathbf{x}_k / \hat{\mathbf{x}}_{k/k-1}) = \begin{bmatrix} \mathbf{1} & \mathbf{0} & \mathbf{0} \\ \hat{\mathbf{x}}_{k/k-1}(2) & \hat{\mathbf{x}}_{k/k-1}(1) & -\mathbf{1} \\ \mathbf{0} & \mathbf{1} & \mathbf{0} \end{bmatrix} \text{ --- (16)}$$

$$\frac{\partial \mathbf{f}}{\partial \hat{\mathbf{x}}} | (\mathbf{x}_k / \hat{\mathbf{x}}_{k/k-1}) = [\hat{\mathbf{x}}_{k/k-1}(2) \quad \hat{\mathbf{x}}_{k/k-1}(1) \quad -\mathbf{1}] \text{ --- (17)}$$

Here, \mathbf{Q}_0 and \mathbf{R}_0 are the covariance frameworks related with the cycle clamor (wk) and the estimation commotion (i.e. ε_k). The \mathbf{R}_0 and \mathbf{Q}_0 for EKF, are regularly introduced as 10^{-4} and $10^{-4}/3 \times 3$, individually [29].

In (13), however, $\mathbf{R}_k = \mathbf{R}_0 e^{\left\| \mathbf{y}_k - \mathbf{g}(\hat{\mathbf{x}}_{k/k-1}) \right\|^2}$ is considered rather than \mathbf{R}_0 , by doling out the remarkable term of mistake between detected burden current and assessed central burden segment, to the blunder covariance term. In the event that the blunder among detected and assessed parts, is high, at that point, the remarkable factor increments quicker, which expands the mistake covariance term and moderation of blunder is accomplished. In this way, vigorous execution of the EKF, is accomplished by consolidating dramatic term, under high unsettling influences in the heap current.

The state forecast is utilized to process the incentive at time point k dependent on the assessed an incentive at time point k-1. In the event that current

elements are generally differed at time point $k-1$, the assessor isn't fit to follow the circumstance and gives fitting weighting. Subsequently, it isn't fit to anticipate a worth that is near the genuine incentive at time point k . In any case, the calculation actually yields the suitable worth, on the grounds that the development vector $(y_k - g(\hat{x}_{k/k-1}))$ quickly changes under such conditions, enhancing the Kalman pick up. The assessed three stages key burden flows $\hat{x}_{k/k,a}(2), \hat{x}_{k/k,b}(2), \hat{x}_{k/k,c}(2)$ are accordingly gotten and prepared further to produce the exchanging beats of VSI. The square chart speaking to the cycle is appeared in Fig. 3.2

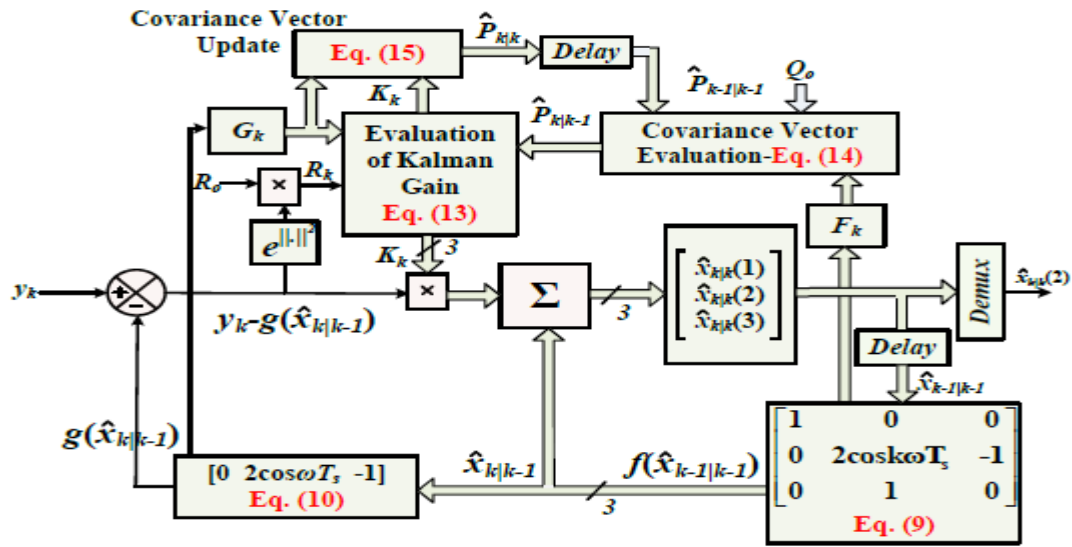


Fig. 3 .2 Implementation of EKF algorithms

As portrayed before, the assessed state vector $\hat{x}_k|k$ from (12), is assessed for k th moment, is the yield of the EKF control. Its deviation from the genuine state vector at k th moment (x_k) is the mistake, for example.

$$e_{k/k} = x_k - \hat{x}_{k/k} \quad \text{--- (18)}$$

The corresponding error at $(k-1)$ th instant can be identified as,

$$e_{k/k-1} = x_k - \hat{x}_{k/k-1} \quad \text{--- (19)}$$

From (11)-(12), the formulations (18)-(19) are as,

$$e_{k/k} = \tilde{F}_{k-1} e_{k/k-1} + n_k + l_k \quad \text{--- (20)}$$

$$e_{k/k-1} = F_{k-1} e_{k-1/k-1} + w_{k-1} + r_{k-1} \quad \text{--- (21)}$$

Where, r_{k-1} is the remainder term at $(k-1)$ th instant $(e_k - F_{k-1} (I_{3 \times 3} - K_k G_{k-1}) e_{k-1})$ and

$$\tilde{F}_{k-1} = [I_{3 \times 3} - (I_{3 \times 3} - K_k G_{k-1}) e_{k-1}] \quad \text{--- (22)}$$

$$n_k = (I_{3 \times 3} - K_k G_{k-1}) w_{k-1} - K_k \varepsilon_k \quad \text{--- (23)}$$

$$l_k = (I_{3 \times 3} - K_k G_{k-1}) r_{k-1} \quad \text{--- (24)}$$

$$\mathbf{F}_{k-1} = \frac{\partial f}{\partial \hat{\mathbf{x}}} |(\hat{\mathbf{x}}_{k/k-1}); \mathbf{G}_{k-1} = \frac{\partial g}{\partial \hat{\mathbf{x}}} |(\hat{\mathbf{x}}_{k/k-1}) \dots (25)$$

With the decent assumptions that the norm $\|\mathbf{F}_k\|$ is bounded and $\hat{\mathbf{P}}_{k/k}$ and $\hat{\mathbf{P}}_{k/k-1}$ are bounded with $\mathbf{P}_1 \mathbf{I}_{3 \times 3}$, $\mathbf{P}_2 \mathbf{I}_{3 \times 3}$ and $\mathbf{q}_1 \mathbf{I}_{3 \times 3}$, $\mathbf{q}_2 \mathbf{I}_{3 \times 3}$ as respective lower and upper bounds. The following lemmas can be identified to prove the exponential convergence of the algorithm [30].

Lemma-1: With \mathbf{F}_k as non-singular $\forall k > 0$, and $\|\mathbf{F}_k\|$, $\hat{\mathbf{P}}_{k/k}$ and $\hat{\mathbf{P}}_{k/k} - \mathbf{1}$ are bounded, then there exist a real number $0 < \lambda < 1$ such that,

$$\tilde{\mathbf{F}}_k^T \mathbf{P}_{k/k-1}^{-1} \tilde{\mathbf{F}}_k \leq (1 - \lambda) \mathbf{P}_{k/k-1}^{-1} \dots (26)$$

Lemma-2: When the ratio of largest and smallest singular value in ' $\mathbf{G}k$ ' matrix has an upper bound 'g', then an upper bound for the norm of the Kalman gain matrix is given as,

$$\|\mathbf{F}_k\| \leq g \left(\frac{q_2}{q_1} \right) \dots (27)$$

Thus, when the error at $(k-1)$ th instant i.e. $\|\mathbf{e}_{k-1/k-1}\|$ is bounded, with the bounds (26) and (27), it can be proved that the solution of the error model (20) is exponentially stable with finite bounded limits [30].

B. Assigning Load Current Weights

The dynamic force segment of burden flows is then assessed utilizing an example and hold (S/H) control rationale. The crucial part assessed from (8)- (17), is gone through S/H rationales. Since the key segment is in stage with the network voltages, the settings off heartbeats for S/H rationales are created utilizing quadrature unit layouts, with a zero intersection indicator (ZCD). This is portrayed in Fig. 3.1. For this reason, the in-stage (xpa,xpb,xpc) and quadrature (xqa,xqb,xqc) unit layouts are registered. To accomplish palatable execution under matrix voltage irregular characteristics and symphonious mutilations, another strategy for extraction of unit formats, is introduced here. The numerical definition for induction of upgraded unit formats follows the accompanying grouping.

- 1) At first the positive succession stage voltages are assessed. The quick certain succession voltage segments in $\alpha\beta$ reference outline are assessed as,

$$\mathbf{V}_{\alpha\beta}^+ = [\mathbf{T}_{\alpha\beta}] [\mathbf{T}_p] [\mathbf{T}_{\alpha\beta}]^1 \mathbf{V}_{\alpha\beta} = \frac{1}{2} \begin{bmatrix} \mathbf{1} & -e^{-j\pi/2} \\ e^{-j\pi/2} & \mathbf{1} \end{bmatrix} \mathbf{V}_{\alpha\beta} \dots (28)$$

$$[\mathbf{T}_{\alpha\beta}] = \sqrt{2/3} \begin{bmatrix} \mathbf{1} & -0.5 & -0.5 \\ 0 & 0.866 & -0.866 \end{bmatrix} \dots (29)$$

$$[T_p] = \frac{1}{3} \begin{bmatrix} 1 & a & a^2 \\ a^2 & 1 & 1 \\ a & a^2 & 1 \end{bmatrix}; a = e^{j2\pi/3} \text{ --- (30)}$$

In this way, from (28) the positive arrangement voltages ' $V_{\alpha\beta}^+$ ' and relating amounts in abc-area, are assessed utilizing reverse Clarke's change. The execution of (28) is portrayed in Fig. 3.3 Initially, $\alpha\beta$ -parts of stage voltages (v_α, v_β) are created through Clarke's change. These are handled through summed up integrators of second request, to get relating in-stage ($v_{\alpha i}, v_{\beta i}$) and quadrature ($v_{\alpha q}, v_{\beta q}$) parts. The depiction of second request second request summed up integrators (SO-SOGI) is accounted for in [31]. The in-stage and quadrature parts are additionally had, as appeared in Fig. 4, to assess the reasonable positive grouping voltage components ($v_{sa} + , v_{sb} + , v_{sc} +$).

- 2) The amplitude of terminal voltage is then evaluated as,

$$V_t = \sqrt{\left(\frac{2}{3}\right) v_{sa}^{+2} + v_{sb}^{+2} + v_{sc}^{+2}} \text{ --- (31)}$$

- 3) The enhanced in-phase ($x_{pa}^m, x_{pb}^m, x_{pc}^m$) and quadrature ($x_{qa}^m, x_{qb}^m, x_{qc}^m$) unit templates are then computed as,

$$x_p^m = [x_{pa}^m \quad x_{pb}^m \quad x_{pc}^m]^T = \left(\frac{1}{V_t}\right) [v_{sa}^+ \quad v_{sb}^+ \quad v_{sc}^+]^T \text{ --- (32)}$$

$$x_q^m = \begin{bmatrix} x_{qa}^m \\ x_{qb}^m \\ x_{qc}^m \end{bmatrix} = \frac{1}{2\sqrt{3}} \begin{bmatrix} 0 & -2 & 2 \\ 3 & 1 & -1 \\ 3 & 1 & -1 \end{bmatrix} \begin{bmatrix} x_{pa}^m \\ x_{pb}^m \\ x_{pc}^m \end{bmatrix} \text{ --- (33)}$$

At last, the heap current loads (WLa, WLb, WLe) are acquired from S/H rationales yield. The normal of burden current weight, is the identical dynamic force segment of burden current ($WLeq$).

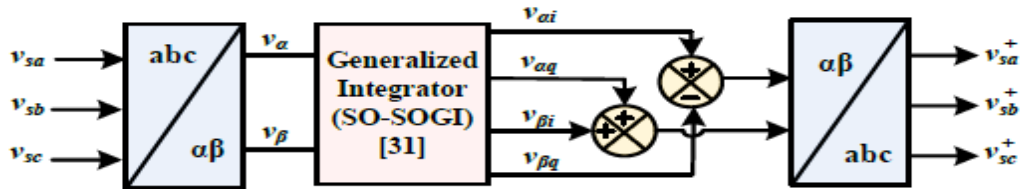


Fig. 3.3 Evaluation of balanced positive sequence grid voltages

C. DC Link Voltage Regulation and PV Feed-Forward Compensation

The PV inverter requires dynamic capacity to direct DC connect voltage (VDC) to its reference (VDC_{ref}). The VSC devours some force from normal coupling point during variety of the DC interface voltage, which is called as misfortune segment of

dynamic power(***W_{loss}***). It is utilized to control DC connect voltage as indicated by reference DC interface voltage, and is assessed as,

$$w_{loss} = K_p(V_{DC}^{ref} - V_{DC}) + K_i \int (V_{DC}^{ref} - V_{DC}) dt \text{ --- (34)}$$

Where, '***kp***' and '***ki***' are the relative and fundamental increases of the regulator, separately. The reference voltage for DC connect capacitor is kept 1.2 occasions the pinnacle of line voltage. Moreover, PV feed-forward term is fused here, to stimulate the dynamic reaction under persistent sun based insolation changes that happen in functional PV framework. A down to earth matrix interfaced PV framework is dependent upon consistent variety of sun oriented segregation. A quick powerful reaction is wanted under such nonstop aggravations to the framework. This is encouraged by the feed-forward term (WPV) by limiting the homeless people in the framework flows. The PV feed-forward is an extra term obliged in the control system, which changes the reference network flows with no criticism from the regulator, to improve the dynamic exhibition of matrix flows during the progressions in sun based insolation. Since the elements are straightforwardly connected with the change in PV cluster power (***P_{PV}***), '***W_{PV}***' can be identified as,

$$W_{PV} = \frac{2P_{PV}}{3V_t} \text{ --- (35)}$$

D. Fault Ride-Through Control

The proposed flaw ride-through control of PV inverter is exhibited in this part. The three stage voltages are communicated in $\alpha\beta$ reference outline utilizing Clarke's change network portrayed in (36) (where ***u $\alpha\beta$*** is vector in $\alpha\beta$ reference frame and ***u_{abc}*** is vector in ***abc*** reference frame),

$$u_{\alpha\beta} = T_{\alpha\beta}^{abc} u_{abc}; T_{abc}^{\alpha\beta} = \sqrt{2/3} \begin{bmatrix} 1 & -1/2 & -1/2 \\ 0 & \sqrt{3}/2 & -\sqrt{3}/2 \end{bmatrix} \text{ --- (36)}$$

The $\alpha\beta$ -voltage components, '***v α*** ' and '***v β*** ' are used to compute their respective positive and negative sequence voltages as follows,

$$\begin{bmatrix} V_{\alpha}^{+} \\ V_{\beta}^{+} \\ V_{\alpha}^{-} \\ V_{\beta}^{-} \end{bmatrix} = \frac{1}{2} \begin{bmatrix} 1 & -e^{-j\pi/2} \\ e^{-j\pi/2} & 1 \\ 1 & e^{-j\pi/2} \\ -e^{-j\pi/2} & 1 \end{bmatrix} \begin{bmatrix} 1 & -1/2 & -1/2 \\ 0 & \sqrt{3}/2 & -\sqrt{3}/2 \end{bmatrix} \begin{bmatrix} V_{sa} \\ V_{sb} \\ V_{sc} \end{bmatrix} \text{ --- (37)}$$

The positive sequence voltage (***V⁺***), negative sequence voltage (***V⁻***) and the per-unit voltage (***V_{pu}***) are then computed as follows, $V^{+} = \sqrt{V_{\alpha}^{+2} + V_{\beta}^{+2}}; V^{-} = \sqrt{V_{\alpha}^{-2} + V_{\beta}^{-2}}$

$$V^+ = (\sqrt{3}/\sqrt{2}V_n)\sqrt{V_{\alpha}^{+2} + V_{\beta}^{+2}}; \bar{V}_{pu} = \text{Mean}(V_{pu}) \text{-----} (38)$$

Where 'Vn' is the ostensible converter voltage. The over flows caused due to the close to PCC shortcomings, trip the interfacing power converter in this manner prompting the misfortune in whole sun based PV age. To evade such disappointments, inverter ostensible force should be refreshed under low voltages. Thusly, a changed ostensible force (MNP) [23], is received here, which is a component of voltage list profundity and ostensible converter power (Sn) as,

$$MNP = \left(\frac{1}{V_n}\right)(V^+ - V^-)S_n \text{-----} (39)$$

Under low voltage flaws in the framework, the altered force is refreshed to take a worth lower than the ostensible intensity of the converter. The decline in voltage sizes of either single stage, twofold stage or three stage voltages, brings about a lessening in the estimation of MNP. This is shown in more definite in the reproduction results. According to the profundity of voltage drop, the assessed receptive force entering the matrix (Q_{gE}) to be provided by the converter is chosen as follows [32],

$$Q_{gE} = \begin{cases} 0 & \text{if } \bar{V}_{pu} > 0.9 \\ (1.35 - 1.5V_{pu})S_n & \text{if } 0.2 < \bar{V}_{pu} < 0.9 \\ 1.05S_n & \text{if } \bar{V}_{pu} < 0.2 \end{cases} \text{-----} (40)$$

In this manner the greatest dynamic force infusion, for a given estimation of MNP and responsive force can be distinguished as,

$$P_{max} = \begin{cases} \sqrt{MNP^2 - Q_{gE}^2} & \text{if } MNP > Q_{gE} \\ 0 & \text{if } MNP < Q_{gE} \end{cases} \text{-----} (41)$$

Under ordinary conditions, the reference lattice receptive force (Q_{gref}) is 'Q_{gE}', represented by (40), However, under profound voltage droops, the VSI is unequipped for infusing the responsive force higher than the MNP, and subsequently, the converter is made to supply receptive force equivalent to MNP. In this manner,

$$Q_{gref} = \begin{cases} Q_{gE} & \text{if } MNP \geq Q_{gE} \\ MNP & \text{if } MNP < Q_{gE} \end{cases} \text{-----} (42)$$

Subsequently, as long as, the P_{max} for example (41) is higher than the greatest force point reference (P_{ref}) gave by the MPPT regulator, the most extreme force can be infused from the PV cluster to the matrix. As referenced before, an InC calculation [28] is utilized for greatest force point following reason, where the heading of annoyance to

arrive at most extreme force point is chosen by the contrast between the steady conductance ($dIPV/dVPV$) and the conductance (IPV/VPV) offered by the PV cluster. At the point when the thing that matters is positive, it recognizes the working point as left of the PV bend and attempts move the working point to one side. The visa-versa is valid for the situation when the thing that matters is negative. Along these lines, the reference PV cluster voltage is assessed dependent on the InC rule the comparing obligation proportion of the lift converter is assessed. Nonetheless, on the off chance tha Pmax is lower than the Pref, at that point the PV exhibit is made to work in de-evaluated mode, at another working point relating to another estimation of dynamic force for example Pmax. The de-appraised activity of PV cluster is portrayed in Fig. 3.4, where the lift converter is controlled to work in non-MPPT mode. As appeared in Fig. 3.4,

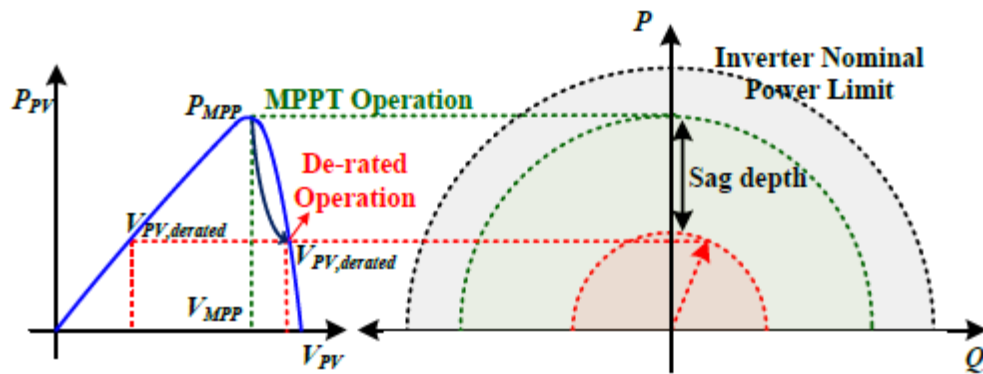


Fig. 3.4 De-rated operation of PV inverter during fault ride-through operation

The right hand side working point is considered here, as the working point can move quicker on the high slope side of the P-V bend. The reference obligation proportion of the lift converter is subsequently gotten under ordinary and de-evaluated conditions as follows,,

$$D_{normal} = 1 - \left(\frac{V_{PV}^{ref}}{V_{DC}} \right) \text{ --- (43)}$$

$$D_{derated} = \left(\frac{P_{max}}{P_{ref}} \right) \left(1 - \left(\frac{V_{PV}^{ref}}{V_{DC}} \right) \right) \text{ --- (44)}$$

Where 'VPV ref ' is the reference PV-cluster voltage gave by the MPPT regulator. The control of the lift converter is exhibited in Fig. 3.5 Under typical conditions, the lift converter is made to work in MPPT mode. Nonetheless, the de-appraised operational mode is enacted when low voltage is recognized (beneath 0.9pu) and $P_{max} < P_{ref}$. The

obligation proportion accordingly got, is contrasted and the high recurrence transporter signal for the age of changing heartbeats to the lift converter. The relative basic regulator in de-appraised activity, tunes new obligation cycle to accurately follow 'Pmax'.

E. Generation of Inverter Gating Pulses

The gating beats for PV inverter are produced utilizing dynamic and receptive reference lattice flows. For this reason, the net dynamic force part (W_{net}) is assessed. The net dynamic force part of current segment is sufficiency of reference lattice flows. This is assessed by summation of equal burden dynamic force part weight with the adequacy of reference inverter flows (45), as per the Kirchhoff current law at PCC. Subsequently ' W_{net} ' can be distinguished as,

$$W_{net} = W_{eq} + W_{loss} - W_{PV} - - - (45)$$

Since ' W_{net} ' is the net dynamic current weight, the reference dynamic force conveyed by the matrix (P_{gref}) is gotten by multiplying ' W_{net} ' with $\sqrt{3}V_{pu}V_n/\sqrt{2}$. Where, ' V_n ' is the ostensible framework voltage. This is on the grounds that the dynamic current weight (W_{net}) is the pinnacle plentifulness of the dynamic current, for example

$$Pg = \sqrt{3}V_{rms}I_{active,rms} = (\sqrt{3}V_{pu}V_n/\sqrt{2})W_{net}$$

. The active reference currents are then evaluated as,

$$i_p^{ref} = [i_{pa}^{ref} \quad i_{pb}^{ref} \quad i_{pc}^{ref}]^T = W_{net}X_p^m - - - (46)$$

To assess the receptive reference flows, the responsive current weight (W_q) is gotten by scaling the reference receptive force decided from (42) with the extent of terminal voltage. The receptive reference flows are then acquired as

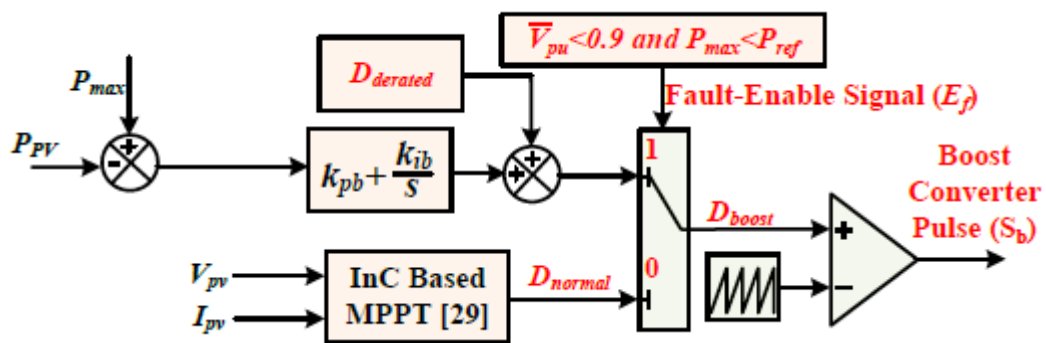


Fig. 3.5 Control schematic for age of lift converter gating beats

$$i_q^{ref} = [i_{qa}^{ref} \quad i_{qb}^{ref} \quad i_{qc}^{ref}]^T = W_qX_q^m - - - (47)$$

Finally, the reference grid currents are generated as,

$$\mathbf{i}_s^{\text{ref}} = \begin{bmatrix} i_{sa}^{\text{ref}} & i_{sb}^{\text{ref}} & i_{sc}^{\text{ref}} \end{bmatrix}^T = i_p^{\text{ref}} + i_q^{\text{ref}} - - - (48)$$

The blunder between reference framework flows (48) and the detected matrix flows is invaded through the hysteresis current regulator (HCC) to deliver the inverter gating beats. The hysteresis band-width (δ) is accounted for in Appendix..

CHAPTER 4

FUZZY LOGIC CONTROLLER

Fuzzy logic is a complex mathematical method that allows solving difficult simulated problems with many inputs and output variables. Fuzzy logic is able to give results in the form of recommendation for a specific interval of output state, so it is essential that this mathematical method is strictly distinguished from the more familiar logics, such as Boolean algebra. This paper contains a basic overview of the principles of fuzzy.

4.1. Fuzzy Logic System

Today control systems are usually described by mathematical models that follow the laws of physics, stochastic models or models which have emerged from mathematical logic. A general difficulty of such constructed model is how to move from a given problem to a proper mathematical model. Undoubtedly, today's advanced computer technology makes it possible; however managing such systems is still too complex.

These complex systems can be simplified by employing a tolerance margin for a reasonable amount of imprecision, vagueness and uncertainty during the modelling phase. As an outcome, not completely perfect system comes to existence; nevertheless in most of the cases it is capable of solving the problem in appropriate way. Even missing input information has already turned out to be satisfactory in knowledge-based systems.

Fuzzy logic allows to lower complexity by allowing the use of imperfect information in sensible way. It can be implemented in hardware, software, or a combination of both. In other words, fuzzy logic approach to problems' control mimics how a person would make decisions, only much faster.

The fuzzy logic analysis and control methods shown in Figure 4.1 can be described as:

Receiving one or large number of measurements or other assessment of conditions existing in some system that will be analysed or controlled.

Processing all received inputs according to human based, fuzzy "if-then" rules, which can be expressed in simple language words, and combined with traditional non-fuzzy processing.

Averaging and weighting the results from all the individual rules into one single output decision or signal which decides what to do or tells a controlled system what to do. The result output signal is a precise defuzzified value.

The following is Fuzzy Logic Control/Analysis Method diagram.

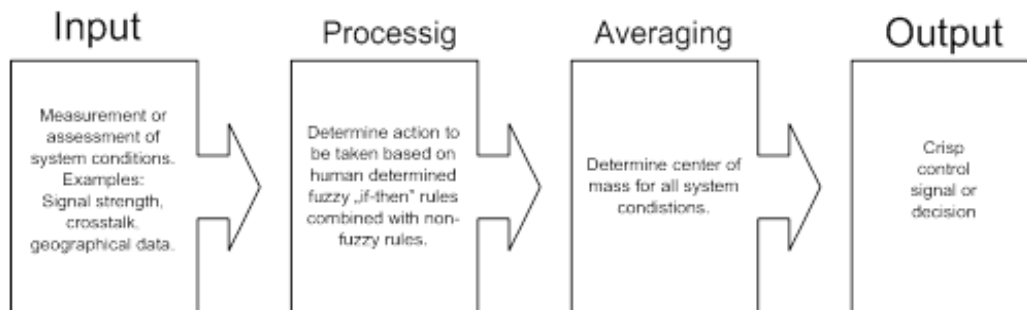


Figure 4.1. The fuzzy logic Control-Analysis method

In order to operate fuzzy logic needs to be represented by numbers or descriptions. For example, speed can be represented by value 5 m/s or by description “slow”. Term “slow” can have different meaning if used by different persons and must be interpreted with respect to the observed environment. Some values are easy to classify, while others can be difficult to determine because of human understanding of different situations. One can say “slow”, while other can say “not fast” when describing the same speed. These differences can be distinguished with help of so-called fuzzy sets.

Usually fuzzy logic control system is created from four major elements presented on Figure 4.2: fuzzification interface, fuzzy inference engine, fuzzy rule matrix and defuzzification interface. Each part along with basic fuzzy logic operations will be described in more detail below.

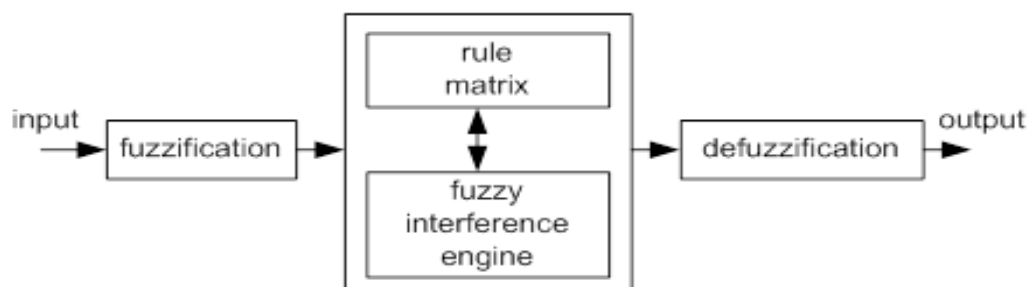


Figure 4.2. Fuzzy logic controller

4.2. Fuzzy Logic Basic Operations

Below some basic information about fuzzy logic will be presented, while a comprehensive theory of fuzzy logic can be found in [2].

• Universe of Discourse

It is a range of all possible values considered as fuzzy system input.

- **Fuzzy Set**

A fuzzy set μ is a function from the reference set X to the unit interval, i.e.

$$\mu: X \rightarrow [0,1] \quad (1)$$

$\mu(X)$ represents the set of all fuzzy sets of X .

- **Membership Function**

It is a graphical representation of fuzzy sets, $\mu_F(x)$.

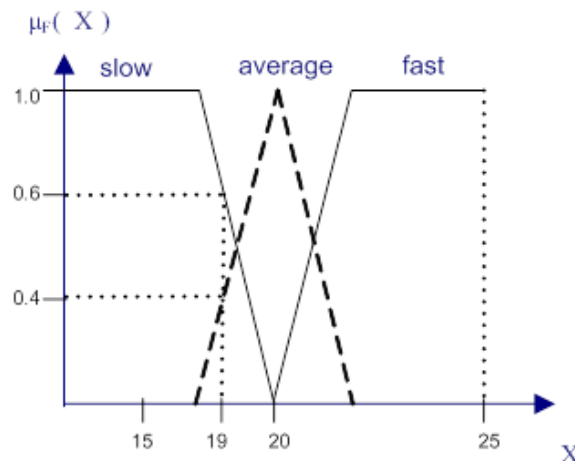


Figure 4.3. An example of fuzzy logic membership function

Figure 4.3 shows the membership functions of three fuzzy sets, “slow”, “average”, and “fast”, for a fuzzy variable Velocity. The universe of discourse creates all possible values of Velocity, i.e., $X = 19$. For Velocity value 19 km/h, the fuzzy set “slow” has the membership value 0.6. Hence, $\mu_{\text{slow}}(19) = 0.6$. Similarly, $\mu_{\text{average}}(19) = 0.4$, and $\mu_{\text{fast}}(19) = 0$.

- **Support**

The support of a fuzzy set F is the crisp set of all points in the Universe of Discourse U such that membership function of F does not equal zero

$$\mu_F(u) > 0 \quad (2)$$

- **Crossover point**

It is an element in U where its membership function equals 0.5.

- **Centre**

The centre of a fuzzy set F is the point (or points) at which $\mu_F(u)$ achieves its maximum value.

4.3. Fuzzification Method

First phase of fuzzy logic proceeding is to deliver input parameters for given fuzzy system based on which the output result will be calculated. These

parameters are Fuzzifier with use of pre-defined input membership functions, which can have different shapes. The most common are: triangular shape, however bell, trapezoidal, sinusoidal and exponential can be also used. Simpler functions will not require complex computing and will not overload the implementation. The degree of membership function is determined by placing a chosen input variable on the horizontal axis, while vertical axis shows quantification of grade of membership of the input variable. The only condition a membership function must meet is that it must vary between zero and one. The value zero means that input variable is not a member of the fuzzy set, while the value one means that input variable is fully a member of the fuzzy set.

With each input parameter there is a unique membership function associated. The membership functions associate a weighting factor with values of each input and the effective rules. These weighting factors determine the degree of influence or degree of membership (DOM) each active rule has. By computing the logical product of the membership weights for each active rule, a set of fuzzy output response magnitudes are produced. All that remains is to combine and defuzzify these output responses.

4.4. Rule Matrix

The rule matrix is used to describe fuzzy sets and fuzzy operators in form of conditional statements. A single fuzzy if-then rule can be as follows

If x is A then y is Z,

Where A is a set of conditions that have to be satisfied and Z is a set of consequences that can be inferred.

In rule with multiple parts, fuzzy operators are used to combine more than one input: AND = min, OR = max and NOT = additive complement. Geometrical demonstration of fuzzy operators is shown in Figure 4.4.

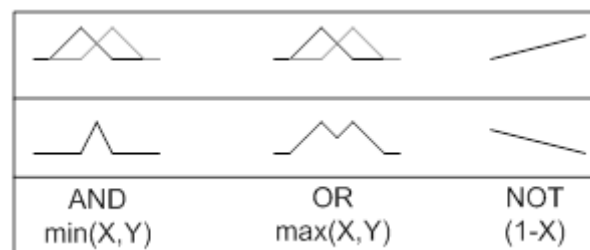


Figure 4.4. Graphical interpretation of fuzzy operators

The rule matrix is a simple graphical tool for mapping the fuzzy logic control system rules. It accommodates two or more input variables and expresses their logical product (AND or OR) as one output response variable. The degree of membership for rule matrix output can take value of maximum, minimum of the degree of previous of the

rule. It is often probable, that after evaluation of all the rules applicable to the input, we get more than one value for the degree of membership. In this case, the simulation has to take into consideration, all three possibilities, the minimum, the maximum or an average of the membership-degrees.

4.5. Inference Mechanisms

Inference mechanism allows mapping given input to an output using fuzzy logic. It uses all pieces described in previous sections: membership functions, logical operations and if-then rules. The most common types of inference systems are Mamdani and Sugeno. They vary in ways of determining outputs.

Mamdani method

Below examples are based on two fuzzy control rules in the form of

R1:if x is A1 and y is B1 then z is C1

R2: if x is A2 and y is B2 then z is C2

Result: z is C, where x equals x0 and y equals y0.

The firing levels of the rules, denoted by α_i , $i = 1, 2$ are calculated by

$$\alpha_1 = A_1(x_0) \wedge B_1(y_0) \quad (3)$$

$$\alpha_2 = A_2(x_0) \wedge B_2(y_0) \quad (4)$$

The individual rule outputs are derived by

$$C'_1(\omega) = (\alpha_1 \wedge C_1(\omega)) \quad (5)$$

$$C'_2(\omega) = (\alpha_2 \wedge C_2(\omega)) \quad (6)$$

Then the overall system output is calculated by oring the individual rule outputs

$$C(\omega) = C'_1(\omega) \vee C'_2(\omega) = (\alpha_1 \wedge C_1(\omega)) \vee (\alpha_2 \wedge C_2(\omega)) \quad (7)$$

Finally, to obtain a deterministic control action, chosen defuzzification mechanism must be implemented.

Sugeno method

Below examples are based on two fuzzy control rules in the form of

R1:if x is A1 and y is B1 then z is $z_1 = a_1x_1 + b_1y_1$

R2: if x is A2 and y is B2 then z is $z_2 = a_2x_2 + b_2y_2$

Result: z0, where x equals x0 and y equals y0.

The firing levels of the rule are calculated in the same way as in Mamdani method, based on (3) and (4) equations. The individual rule outputs are calculated from the below relationships

$$z_1 = a_1 \cdot x_0 + b_1 \cdot y_0 \quad (8)$$

$$z_2 = a_2 \cdot x_0 + b_2 \cdot y_0 \quad (9)$$

If there is n rules in the rule matrix, the crisp control result derived from the following equations

$$z_0 = \frac{\sum_{i=1}^n \alpha_i z_i}{\sum_{i=1}^n \alpha_i} \quad (10)$$

where α_i is a firing level of the i rule, and $i = 1, \dots, n$.

The Sugeno method works well with linear techniques, as it is computationally efficient. It is suitable to apply optimisation and adaptive techniques. Furthermore, it guarantees continuity of the output surface and it is well suited to mathematical analysis. An advantage of the Mamdani method is that it is intuitive and has widespread acceptance. It can be well suited to human input.

4.6. Defuzzification Mechanisms

Defuzzification task is to find one single crisp value that summarises the fuzzy set. There are several mathematical techniques available: centroid, bisector, mean, maximum, maximum and weighted average. Figure 4.5 demonstrate illustration of how values for each method are chosen.

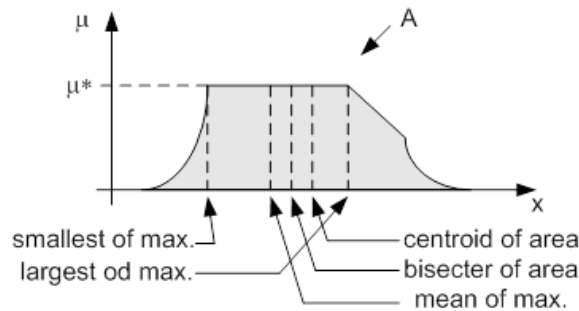


Figure 4.5. Graphical demonstration of defuzzification methods

Centroid defuzzification is the most commonly used method, as it is very accurate. It provides centre of the area under the curve of membership function. For complex membership functions it puts high demands on computation. It can be expressed by the following formula

$$z_0 = \frac{\int \mu_i(x) x dx}{\int \mu_i(x) dx} \quad (11)$$

Where z_0 is defuzzified output, μ_i is a membership function and x is output variable.

Bisector defuzzification uses vertical line that divides area under the curve into two equal areas.

$$\int_{\alpha}^z \mu_A(x) dx = \int_z^{\beta} \mu_A(x) dx \quad (12)$$

Mean of maximum defuzzification method uses the average value of the aggregated membership function outputs.

$$z_0 = \frac{\int_{x'} x dx}{\int_{x'} dx} \quad (13)$$

Where $x' = \{x; \mu_A(x) = \mu^*\}$.

Smallest of maximum defuzzification method uses the minimum value of the aggregated membership function outputs.

$$z_0 \in \left\{ x \mid \mu(x) = \min_{\omega} \mu(\omega) \right\} \quad (14)$$

Largest of maximum defuzzification method uses the maximum value of the aggregated membership function outputs.

$$z_0 \in \left\{ x \mid \mu(x) = \max_{\omega} \mu(\omega) \right\} \quad (15)$$

Weighted average defuzzification method, based on peak value of each fuzzy sets, calculates weighted sum of these peak values [4]. According to these weight values and the degree of membership for fuzzy output, the crisp value of output is determined by the following formula

$$z_0 = \frac{\sum \mu(x)_i \times W_i}{\sum \mu(x)_i} \quad (16)$$

Where μ_i is the degree of membership in output singleton i , W_i and is the fuzzy output weight value for the output singleton

CHAPTER 5

SIMULATION RESULTS

A.Simulation results using pi controller:

To verify the proposed control scheme, a simulation test-bed is built in MATLAB®-Simulink based environment with Sims cape toolbox. A 415V, 50Hz system is considered here, with DC link voltage of 1.2 times the peak of line voltage. This section describes the system performance under grid-side faults, highlighting the salient signals.

The performance of grid interfaced PV system under low voltage faults is depicted in Fig. (5.8_5.11). The simulation parameters are reported in Appendix. Single line to ground (L-G) and double-line to ground (L-L-G) faults, are simulated at 1s and 1.1s, respectively. Upon the occurrence of the fault, the per-unit voltage falls to 0.6pu. A severe L-L-G fault is then simulated at 1.2s where the grid voltages fall as low as 0.1pu. The salient signals of grid voltages (v_g), $V_+ - V_-$, V_{pu} , MNP, P_{max} , Q_g , D normal, Dboost, PPV, VPV, grid currents (i_g) and VSC currents (i_{VSC}) are depicted in Fig. 11. As soon as fault signal is detected by the algorithm, $V_+ - V_-$, MNP and P_{max} are updated as per (38),(39) and (41), respectively. The reactive power injected to the grid, follows the reference reactive power (42), and thereby provides the reactive power support under low voltage faults. As soon as the MNP falls below the rated power of power converter (35 kVA), the de-rated PV array operation mode is enabled. Consequently, the duty ratio is updated as per (43)-(44) (Fig.6). The PI control parameters (k_{pb} and k_{ib}) are reported in Appendix. Accordingly, the dynamics in duty ratio of the boost converter (Dboost), PV voltage (V_{pv}) and PV array power (P_{pv}) are observed . Before the occurrence of the fault, the PV array operates at its MPP of 440V and 30kW, however, the PV power is limited to P_{max} (25kW and 19kW), after the occurrence of faults at 1s and 1.1s, and V_{pv} is shifted to a new operating points at 500V and 522V, respectively. It may be noted from Figs. 5.8-5.11) that, under severe grid faults (at 1.2s), the reactive power entering the grid (Q_g) is limited to MNP (3.5 kVA). In this case, no active power supplied by the PV inverter, with zero duty-ratio of the boost converter; thus, the PV inverter simply acts as a static compensator. Despite the unbalanced voltage faults, the grid currents always remained balanced and sinusoidal with THD less than 5%, as the compensating currents are provided by the PV inverter under all conditions.

Case1: System response under L-G and L-L-G faults depicting fault ride-through operation of PV inverter

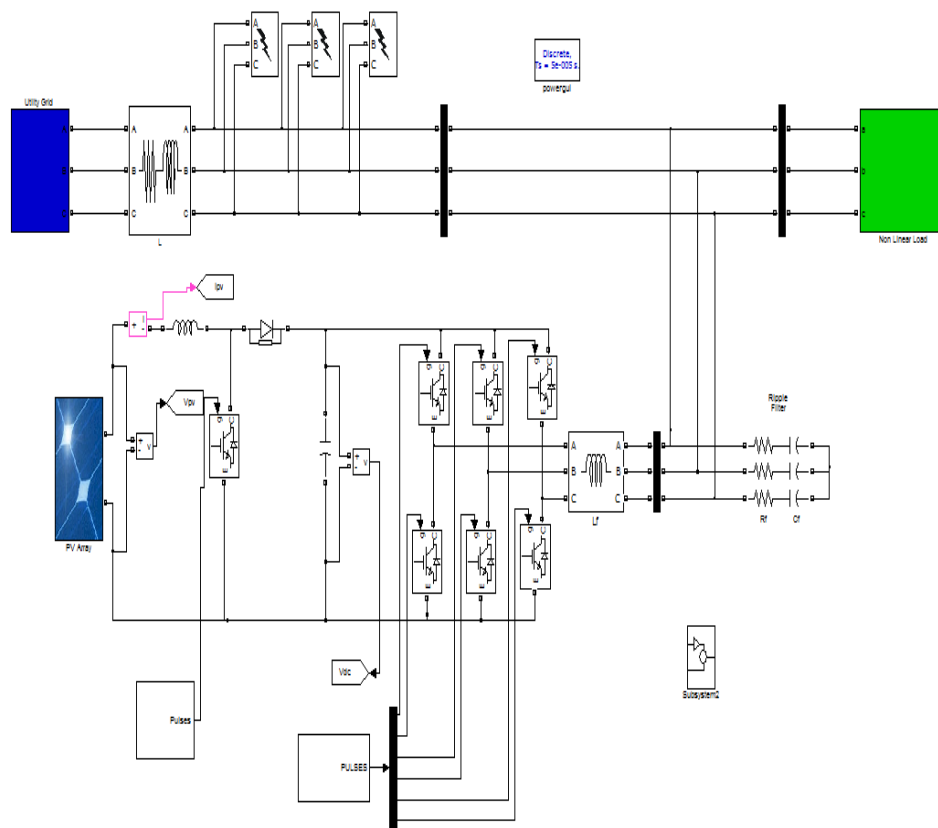


Fig5.1 simulation model by using PI controller

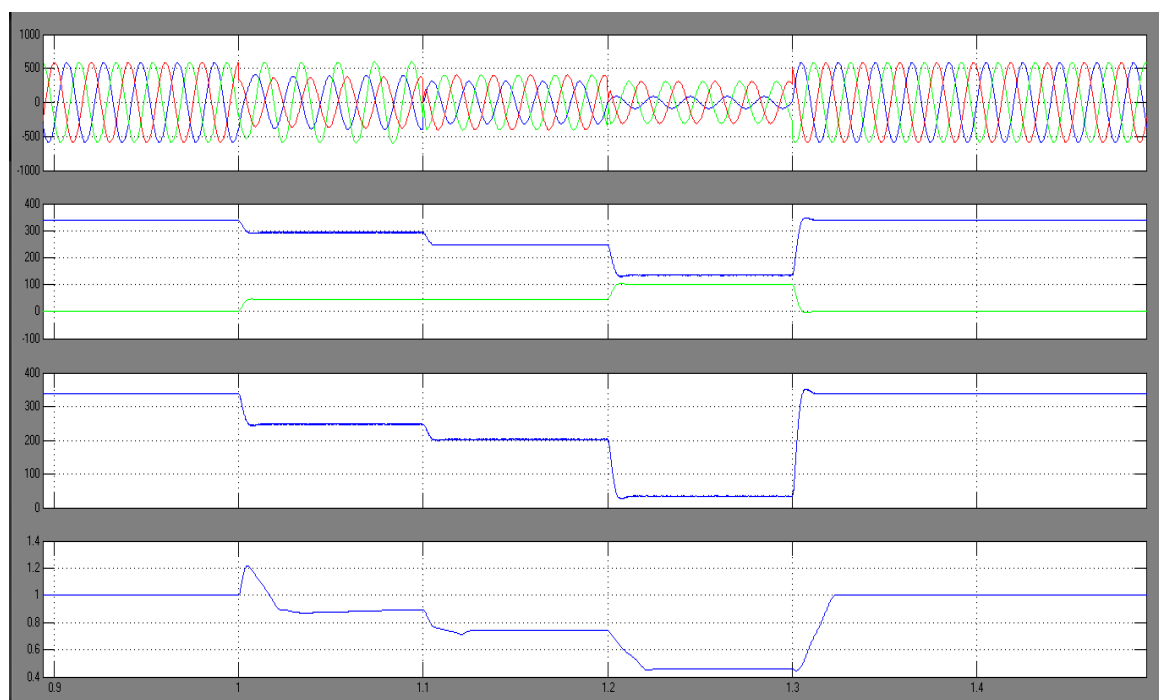


Fig 5.2 V_{sabc} , V^+ & V^- , $V^+ - V^-$, V_{pu}

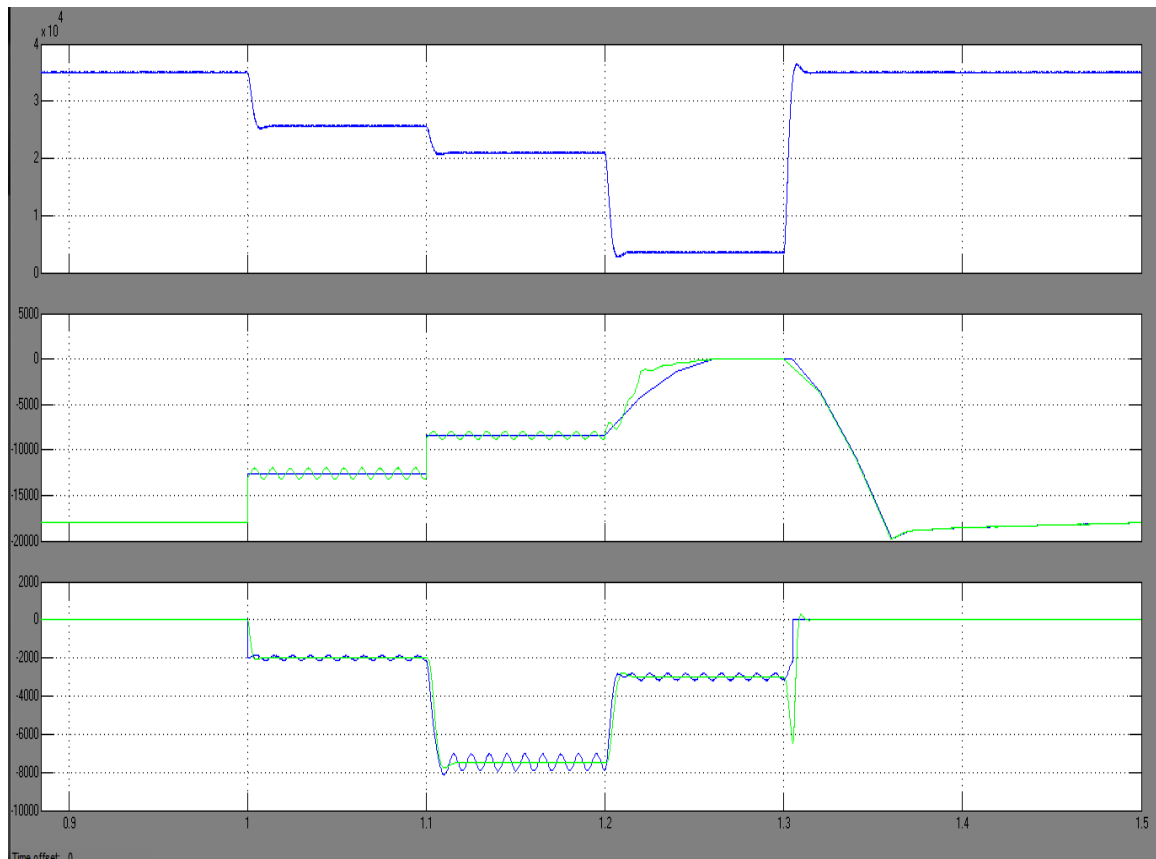


Fig 5.3 MN_p , P_g , Q_g

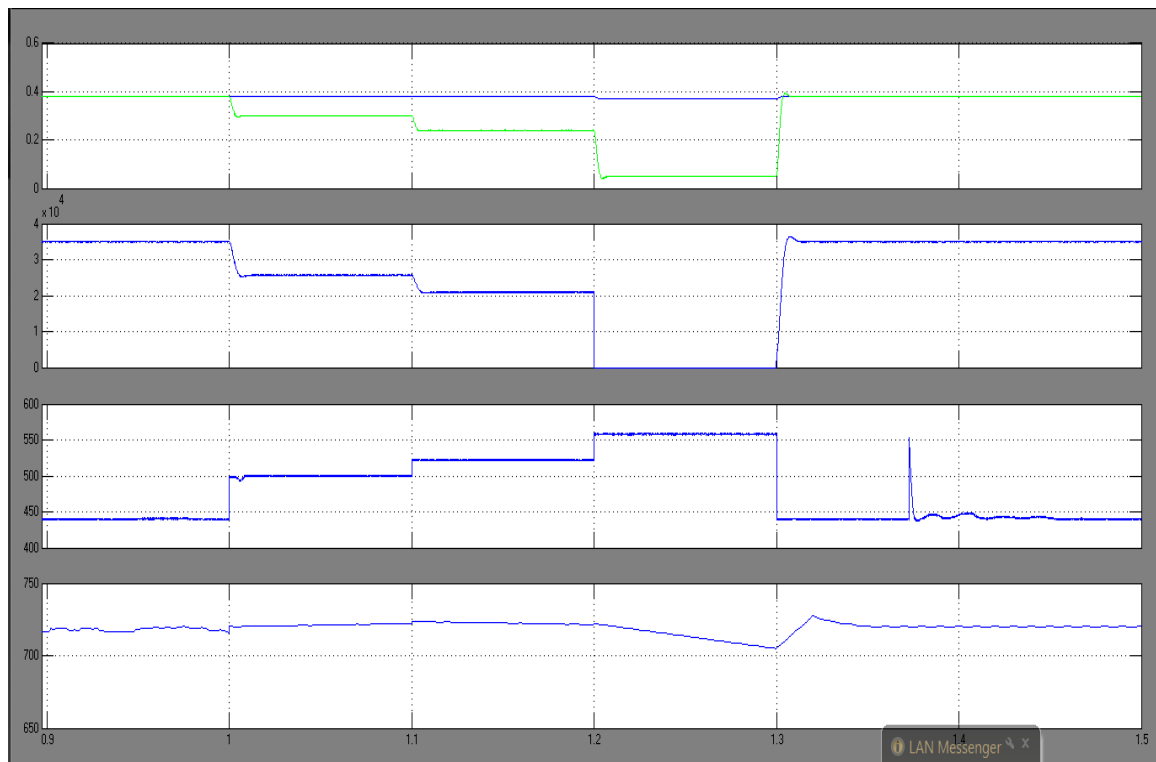


Fig 5.4 D_{boost} , P_{max} , V_{pv} , V_{dc}

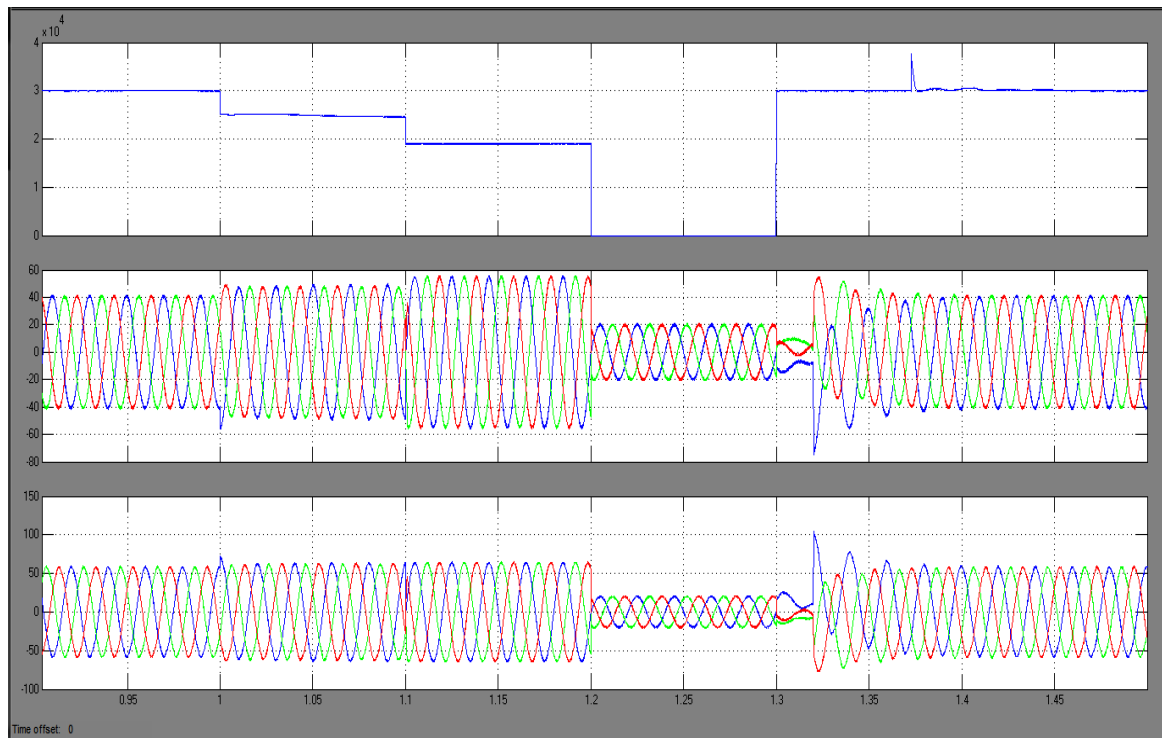


Fig5.5 Ppv, Isabc, Ivsc

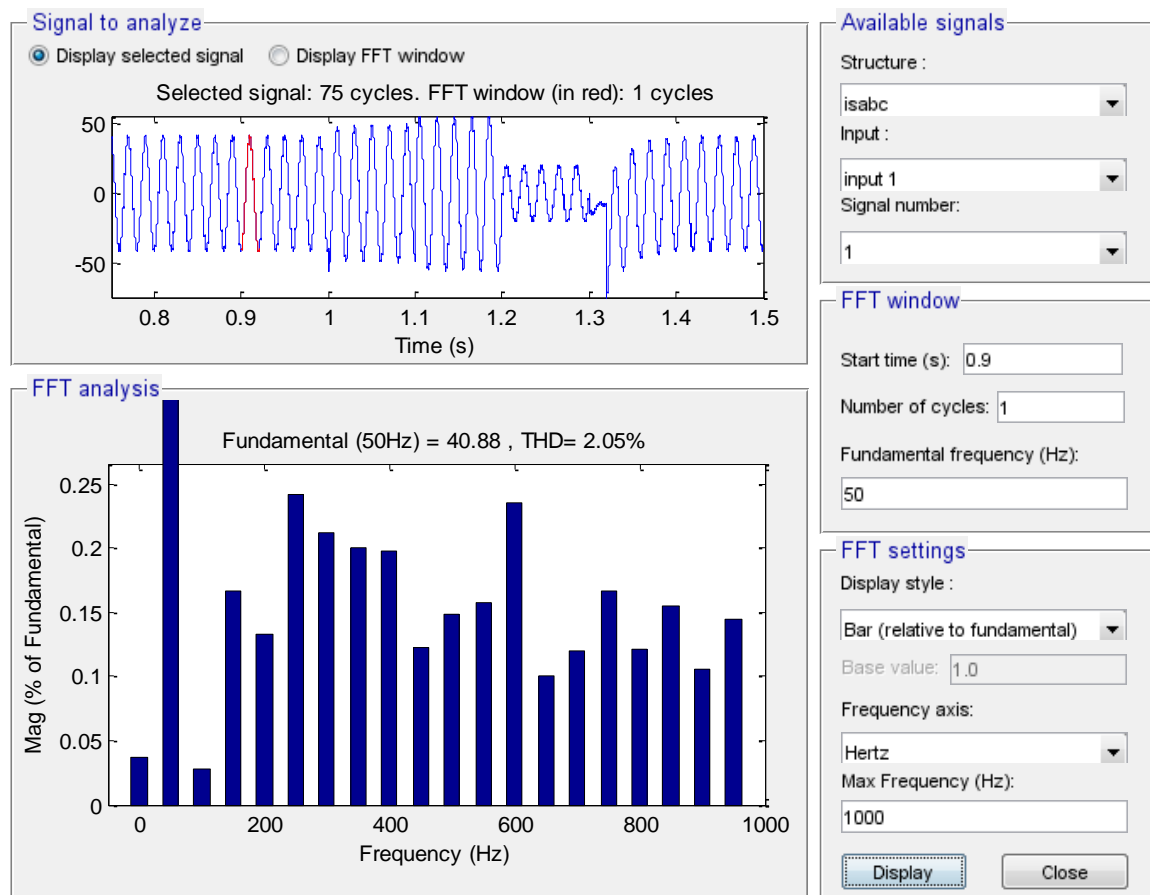


Fig 5.6 THD value of isabc

B. Simulation results using anfis controller:

To verify the proposed control scheme, a simulation test-bed is built in MATLAB®-Simulink based environment with Sims cape toolbox. A 415V, 50Hz system is considered here, with DC link voltage of 1.2 times the peak of line voltage. This section describes the system performance under grid-side faults, highlighting the salient signals.

The performance of grid interfaced PV system under low voltage faults is depicted in Fig. (5.8_5.11). The simulation parameters are reported in Appendix. Single line to ground (L-G) and double-line to ground (L-L-G) faults, are simulated at 1s and 1.1s, respectively. Upon the occurrence of the fault, the per-unit voltage falls to 0.6pu. A severe L-L-G fault is then simulated at 1.2s where the grid voltages fall as low as 0.1pu. The salient signals of grid voltages (v_g), $V^+ - V^-$, V_{pu} , MNP, P_{max} , Q_g , D_{normal} , D_{boost} , PPV, VPV, grid currents (i_g) and VSC currents (i_{VSC}) are depicted in Fig. 11. As soon as fault signal is detected by the algorithm, $V^+ - V^-$, MNP and P_{max} are updated as per (38),(39) and (41), respectively. The reactive power injected to the grid, follows the reference reactive power (42), and thereby provides the reactive power support under low voltage faults. As soon as the MNP falls below the rated power of power converter (35 kVA), the de-rated PV array operation mode is enabled. Consequently, the duty ratio is updated as per (43)-(44) (Fig.6). The PI control parameters (k_{pb} and k_{ib}) are reported in Appendix. Accordingly, the dynamics in duty ratio of the boost converter (D_{boost}), PV voltage (V_{pv}) and PV array power (P_{pv}) are observed. Before the occurrence of the fault, the PV array operates at its MPP of 440V and 30kW, however, the PV power is limited to P_{max} (25kW and 19kW), after the occurrence of faults at 1s and 1.1s, and V_{pv} is shifted to a new operating points at 500V and 522V, respectively. It may be noted from Figs. 5.8-5.11) that, under severe grid faults (at 1.2s), the reactive power entering the grid (Q_g) is limited to MNP (3.5 kVA). In this case, no active power supplied by the PV inverter, with zero duty-ratio of the boost converter; thus, the PV inverter simply acts as a static compensator. Despite the unbalanced voltage faults, the grid currents always remained balanced and sinusoidal with THD less than 5%, as the compensating currents are provided by the PV inverter under all conditions.

Case_2 System response under L-G and L-L-G faults depicting fault ride-through operation of PV inverter

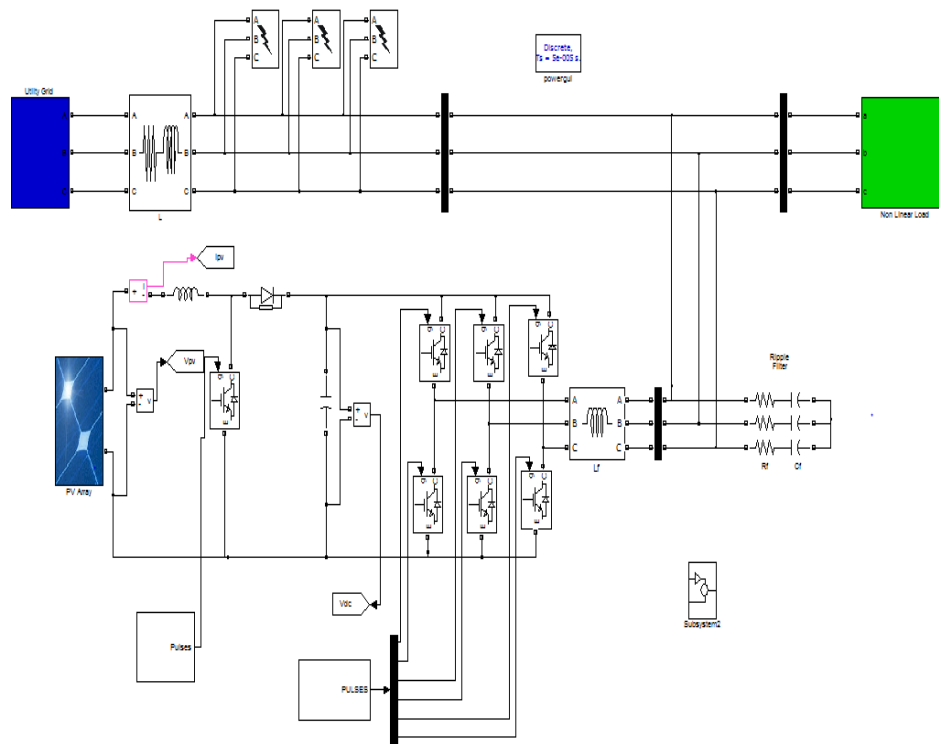


Fig 5.7 Simulation model by using ANFIS Controller

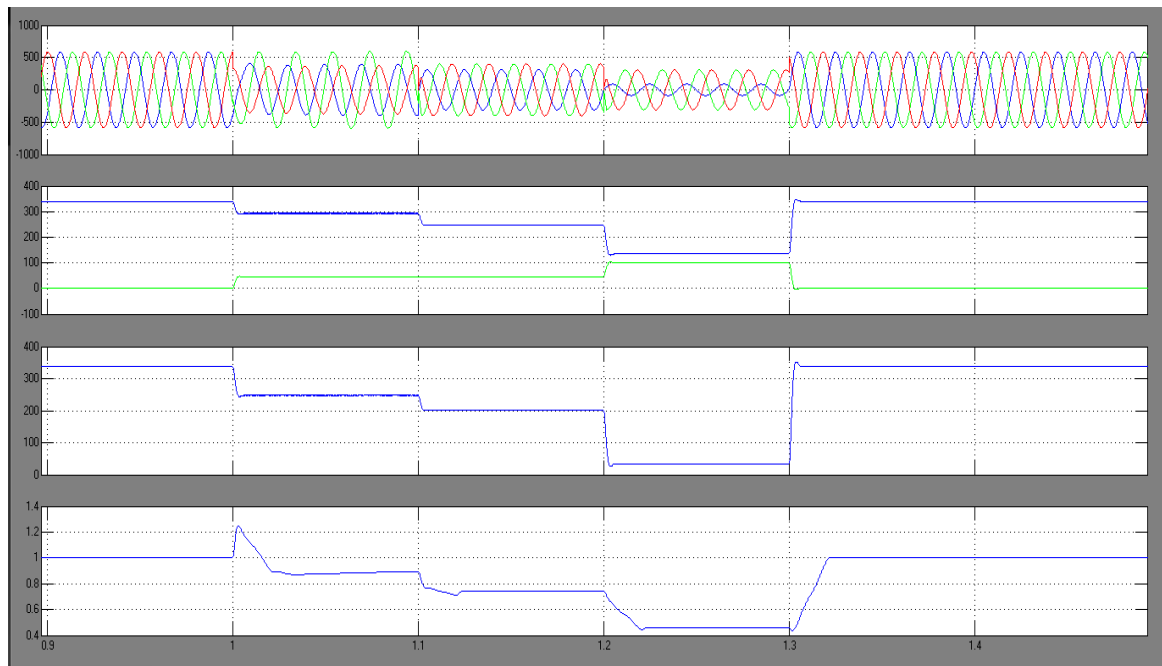


Fig 5.8 V_{sabc} , V^+ & V^- , $V^+ - V^-$, V_{pu}

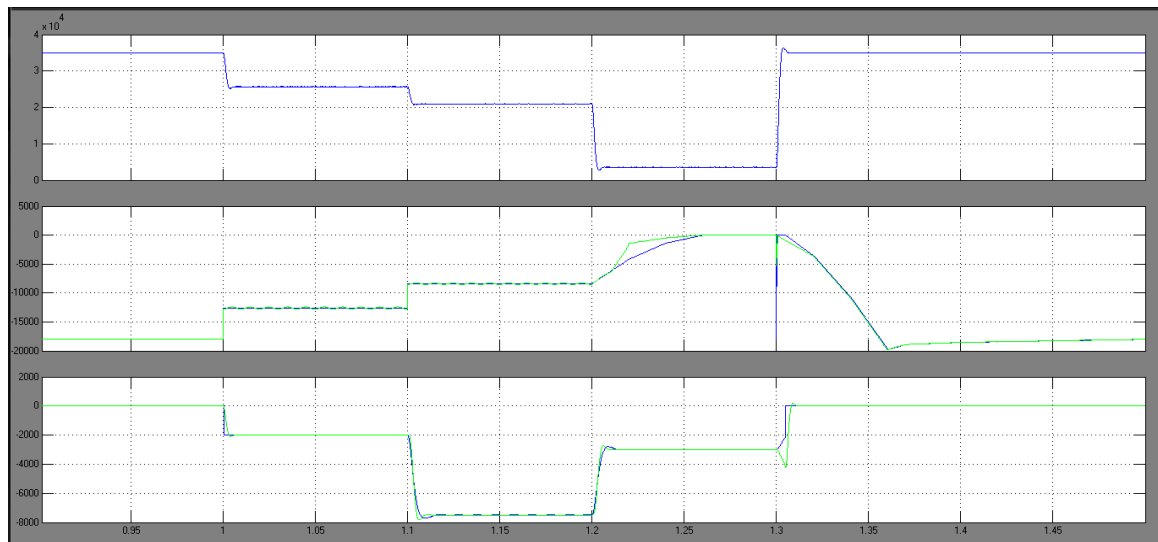


Fig 5.9 MN_p, P_g, Q_g

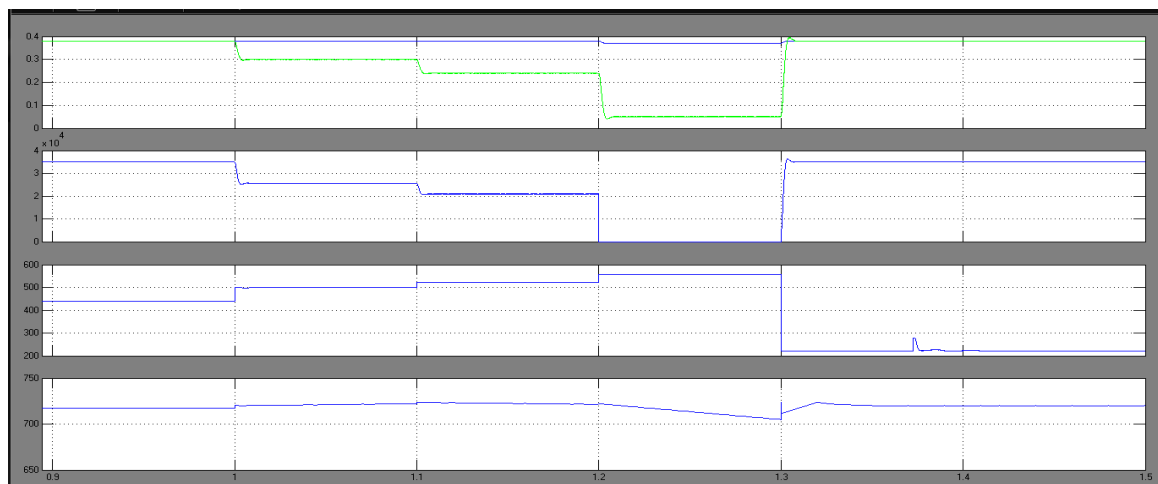


Fig 5.10 Dboost P_{max}, V_{pv}, V_{dc}

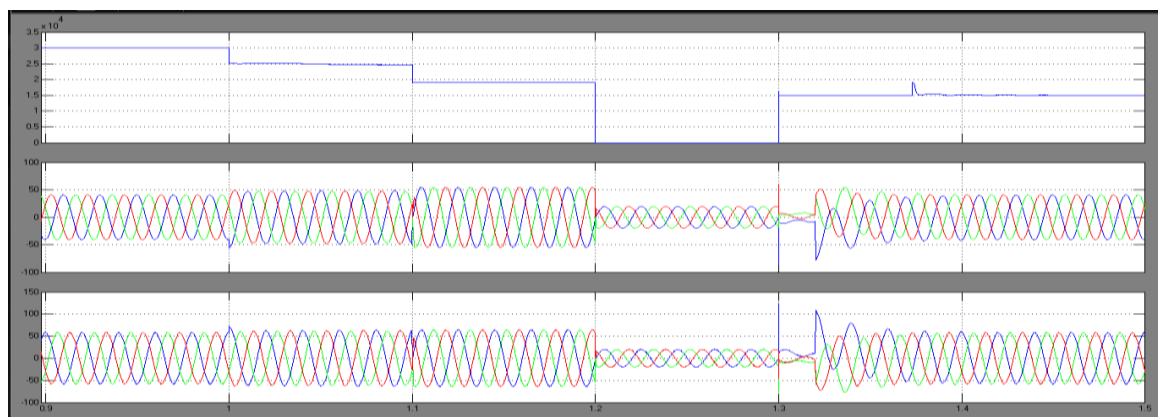


Fig 5.11 $P_{pv}, I_{sabc}, I_{vsc}$

CONCLUSION

The EKF state-estimator based control strategy is proposed for fault ride through operation in two-stage grid interfaced PV system, which enables the load compensation features in three phase distribution system. The converter over-currents caused due to low voltage sags in the GPV system, are avoided, by providing an auxiliary reactive power support as recommended by IEEE Standard-1547.4. Here, the ride-through operation is achieved without compromising the load compensation features such as grid harmonic currents elimination, grid currents balancing and power factor correction. For ride-through purpose, a maximum safe limit of PV power injection is derived as a function of grid-voltage sag and the PV inverter rating. The de-rated operation of PV array is enabled, in cases when the maximum PV power becomes higher than the maximum safe limit of active power injection. To achieve this, the mechanism for a boost converter duty-ratio control, is presented. The reactive power is then injected to the grid under voltage sag faults, as per the depth in voltage-sag.

The simulation results under LG and LLG faults, demonstrate the effectiveness of proposed control scheme. Despite the unbalanced faults, the grid currents remain balanced and sinusoidal, thereby, the negative sequence and zero sequence power injection to the grid are avoided. Test results validate proposed control strategy. The features of harmonic currents mitigation, reactive power compensation, grid currents balancing and power factor correction, are illustrated under various test conditions. The results under distorted grid voltages and L-G unbalanced fault are also presented. Under both normal and abnormal grid conditions, the grid currents with proposed control strategy, are balanced and are maintained within the THD limit recommended by the IEEE standard-519. The practical grid interfaced PV systems, are subject to continuous grid side perturbations and proposed control strategy serves as a possible solution, owing to its multi-functional features and self-adaptation capability to the variations in grid-side parameters.

REFERENCES

- [1] E.Hache, A. Palle, “Renewable energy source integration into power networks, research trends and policy implications: A bibliometric and research actors survey analysis”, *Energy Policy*, vol. 124, pp. 23-35, 2019.
- [2] B. Singh, A. Chandra, and K. Al-Haddad, *Power Quality: Problems and Mitigation Techniques*. Hoboken, NJ, USA: Wiley, Jan. 2015.
- [3] V. L. Srinivas, S. Kumar, S. Bhim and S. Mishra, "A Multifunctional GPV System Using Adaptive Observer Based Harmonic Cancellation Technique," *IEEE Trans.Ind. Electron.*, vol. 65, no. 2, pp. 1347-1357, 2018..
- [4] S. Bhim and J. Solanki, “A comparison of control algorithms for DSTATCOM,” *IEEE Trans. Ind. Electr.*, vol. 56, no. 7, pp. 2738-2745, July 2009.
- [5] Q. Chen, X. Luo, L. Zhang and S. Quan, “Model predictive control for three-phase four-leg grid-tied inverters,” *IEEE Access*, vol. 5, pp. 2834-2841, 2017.
- [6] K. K. Shyu, M. J. Yang, Y. M. Chen and Y. F. Lin, "Model Reference Adaptive Control Design for a Shunt Active Power Filter System," in *Proc. IECON 2006 - 32nd Annual Conference on IEEE Industrial Electronics*, Paris, 2006, pp. 73-78.
- [7] W. Fei, J. L. Duarte, and M. A. M. Hendrix, “Pliant active and reactive power control for grid-interactive converters under unbalanced voltage dips,” *IEEE Trans. Pow. Electr.*, vol. 26, no. 5, pp. 1511–1521, 2011.
- [8] H. S. Song and K. Nam, “Dual current control scheme for PWM converter under unbalanced input voltage conditions,” *IEEE Trans. Ind. Electron.*, vol. 46, no. 5, pp. 953–959, Oct. 1999.
- [9] M. Reyes, P. Rodriguez, S. Vazquez, A. Luna, R. Teodorescu, and J. M. Carrasco, “Enhanced decoupled double synchronous reference frame current controller for unbalanced grid-voltage conditions,” *IEEE Trans. Power Electron.*, vol. 27, no. 9, pp. 3934–3943, Sep. 2012.
- [10] A. Camacho, M. Castilla, J. Miret, A. Borrell, and L. de Vicuna, “Active and reactive power strategies with peak current limitation for distributed generation inverters during unbalanced grid faults,” *IEEE Trans. Ind. Electron.*, vol. 62, no. 3, pp. 1515-1525, Mar. 2015.

- [11] A. Camacho, M. Castilla, J. Miret, J. Vasquez, and E. Alarcon-Gallo, "Flexible voltage support control for three phase distributed generation inverters under grid fault," *IEEE Trans. Ind. Electron.*, vol. 60, no. 4, pp. 1429–1441, 2013.
- [12] J. Miret, A. Camacho, M. Castilla, L. G. de Vicuna, and J. Matas, "Control scheme with voltage support capability for distributed generation inverters under voltage sags," *IEEE Trans. Power Electron.*, vol. 28, no. 11, pp. 5252–5263, Nov. 2013.
- [13] C. T. Lee, C. W. Hsu, and P. T. Cheng, "A low-voltage ride-through technique for grid-connected converters of distributed energy resources," *IEEE Trans. Ind. Appl.*, vol. 47, no. 4, pp. 1821–1832, 2011.
- [14] M. Castilla, J. Miret, A. Camacho, J. Matas, and L. Garcia de Vicuna, "Voltage support control strategies for static synchronous compensators under unbalanced voltage sags," *IEEE Trans. Ind. Electron.*, vol. 61, no. 2, pp. 808–820, Feb. 2014.
- [15] Y. Suh and T. A. Lipo, "Control scheme in hybrid synchronous stationary frame for PWM AC/DC converter under generalized unbalanced operating conditions," *IEEE Trans. Ind. Appl.*, vol. 42, no. 3, pp. 825–835, May/ Jun. 2006.
- [16] Z. Li, Y. Li, P. Wang, H. Zhu, C. Liu, and W. Xu, "Control of three-phase boost-type PWM rectifier in stationary frame under unbalanced input voltage," *IEEE Trans. Power Electron.*, vol. 25, no. 10, pp. 2521–2530, Oct. 2010.
- [17] P. Rodriguez, A. V. Timbus, R. Teodorescu, M. Liserre, and F. Blaabjerg, "Flexible active power control of distributed power generation systems during grid faults," *IEEE Trans. Ind. Electron.*, vol. 54, no. 5, pp. 2583–2592, Oct. 2007.
- [18] F. Wang, J. L. Duarte, and M. A. M. Hendrix, "Pliant active and reactive power control for grid-interactive converters under unbalanced voltage dips," *IEEE Trans. Pow. Electr.*, vol. 26, no. 5, pp. 1511–1521, 2011.
- [19] M. Mir Hosseini, J. Pou, V. G. Agelidis, "Individual phase current control with the capability to avoid overvoltage in grid-connected photovoltaic power plants under unbalanced voltage sags", *IEEE Trans. Power Electron.*, vol. 30, no. 10, pp 5346–5351, 2015.
- [20] Y. Yang, H. Wang, F. Blaabjerg and T. Kerekes, "A Hybrid Power Control Concept for PV Inverters with Reduced Thermal Loading," *IEEE Trans. Pow. Electron.* vol. 29, no. 12, pp. 6271-6275, Dec. 2014.

- [21] H. D. Tafti, A. Maswood, G. Konstantinou, J. Pou, K. Kandasamy, Z. Lim, and G. H. P. Ooi, "Study on the low-voltage ride-through capability of photovoltaic grid-connected neutral-point-clamped inverters with active/reactive power injection," *IET Renew. Pow. Gen.*, vol. 11, pp. 1182–1190, July 2017.
- [22] D. Hossein, A. Iftekhar, K. Georgios, P. Josep and P. Acuna, "Active/reactive power control of photovoltaic grid-tied inverters with peak current limitation and zero active power oscillation during unbalanced voltage sags," *IET Power Electron.*, vol. 11, no. 6, 2018.
- [23] E. Afshari, Gholam R. Moradi, R. Rahimi, B. Farhangi, Y. Yang ; F. Blaabjerg and S. Farhangi, "Control Strategy for Three-Phase Grid-Connected PV Inverters Enabling Current Limitation Under Unbalanced Faults," *IEEE Trans. Ind. Electr.*, vol. 64, no. 11, pp. 8908-8918, 2017.
- [24] N. Zhang, H. Tang, and C. Yao, "A systematic method for designing a PR controller and active damping of the LCL filter for single-phase grid-connected PV inverters", *Energies*, vol.7, no. 6, pp.3934-3954, 2014.
- [25] F. Wu, D. Sun, L. Zhang and J. Duan, "Influence of plugging DC offset estimation integrator in single-phase EPLL and alternative scheme to eliminate effect of input DC offset and harmonics," *IEEE Trans. Ind. Electron.*, vol. 62, no. 8, pp. 4823-4831, Aug. 2015.
- [26] U. Subudhi, H. K. Sahoo and S. K. Mishra, "Harmonics and Decaying DC Estimation Using Volterra LMS/F Algorithm," in *IEEE Trans. Ind. Appl.*, vol. 54, no. 2, pp. 1108-1118, March-April 2018..
- [27] N. Kishor, S. R. Mohanty, M. G. Villalva and E. Ruppert, "Simulation of PV array output power for modified PV cell model," in *Proc. IEEE Int. Conf. on Power and Energy*, Kuala Lumpur, pp. 533-538, 2010.
- [28] M. A. G. de Brito, L. Galotto, L. P. Sampaio, G. d. A. e Melo and C. A. Canesin, "Evaluation of the Main MPPT Techniques for Photovoltaic Applications," in *IEEE Transactions on Industrial Electronics*, vol. 60, no. 3, pp. 1156-1167, March 2013.
- [29] G. Anagnostou and B. C. Pal, "Derivative-Free Kalman Filtering Based Approaches to Dynamic State Estimation for Power Systems With Unknown Inputs," *IEEE Trans. Power Sys.*, vol. 33, no. 1, pp. 116-130, Jan. 2018.

- [30] Knut Rapp, "Nonlinear estimation and control in the iron ore pelletizing process: An application and analysis of the Extended Kalman filter", PhD thesis, Norwegian University of Technology, NTNU, 2004.
- [31] Z. Xin, X. Wang, Z. Qin, M. Lu, P. C. Loh and F. Blaabjerg, "An Improved Second-Order Generalized Integrator Based Quadrature Signal Generator," IEEE Trans. Power Electron., vol. 31, no. 12, pp. 8068-8073, Dec. 2016.